



International Agreement Report

Evaluation for 4-Inch Cold Leg Top-Slot Break LOCA in ATLAS Facility with RELAP5 Mod3.3 Patch5

Prepared by:

J. Kim*, K.-H. Kang*, B.-U. Bae*, Y. Park*, A. Shin**, M. Cho**

*Korea Atomic Energy Research Institute,
111, Daedeok-daero 989beon-gil, Yuseong-gu, Daejeon, Korea

**Korea Institute of Nuclear Safety
62 Gwahak-ro, Yuseong-gu, Daejeon 34142, Republic of Korea

K. Tien, NRC Project Manager

**Division of Systems Analysis
Office of Nuclear Regulatory Research
U.S. Nuclear Regulatory Commission
Washington, DC 20555-0001**

Manuscript Completed: February 2020

Date Published: January 2021

Prepared as part of
The Agreement on Research Participation and Technical Exchange
Under the Thermal-Hydraulic Code Applications and Maintenance Program (CAMP)

**Published by
U.S. Nuclear Regulatory Commission**

AVAILABILITY OF REFERENCE MATERIALS IN NRC PUBLICATIONS

NRC Reference Material

As of November 1999, you may electronically access NUREG-series publications and other NRC records at NRC's Library at www.nrc.gov/reading-rm.html. Publicly released records include, to name a few, NUREG-series publications; *Federal Register* notices; applicant, licensee, and vendor documents and correspondence; NRC correspondence and internal memoranda; bulletins and information notices; inspection and investigative reports; licensee event reports; and Commission papers and their attachments.

NRC publications in the NUREG series, NRC regulations, and Title 10, "Energy," in the *Code of Federal Regulations* may also be purchased from one of these two sources.

1. The Superintendent of Documents

U.S. Government Publishing Office
Mail Stop IDCC
Washington, DC 20402-0001
Internet: bookstore.gpo.gov
Telephone: (202) 512-1800
Fax: (202) 512-2104

2. The National Technical Information Service

5301 Shawnee Road
Alexandria, VA 22312-0002
www.ntis.gov
1-800-553-6847 or, locally, (703) 605-6000

A single copy of each NRC draft report for comment is available free, to the extent of supply, upon written request as follows:

Address: **U.S. Nuclear Regulatory Commission**
Office of Administration
Multimedia, Graphics, and Storage &
Distribution Branch
Washington, DC 20555-0001
E-mail: distribution.resource@nrc.gov
Facsimile: (301) 415-2289

Some publications in the NUREG series that are posted at NRC's Web site address www.nrc.gov/reading-rm/doc-collections/nuregs are updated periodically and may differ from the last printed version. Although references to material found on a Web site bear the date the material was accessed, the material available on the date cited may subsequently be removed from the site.

Non-NRC Reference Material

Documents available from public and special technical libraries include all open literature items, such as books, journal articles, transactions, *Federal Register* notices, Federal and State legislation, and congressional reports. Such documents as theses, dissertations, foreign reports and translations, and non-NRC conference proceedings may be purchased from their sponsoring organization.

Copies of industry codes and standards used in a substantive manner in the NRC regulatory process are maintained at—

The NRC Technical Library

Two White Flint North
11545 Rockville Pike
Rockville, MD 20852-2738

These standards are available in the library for reference use by the public. Codes and standards are usually copyrighted and may be purchased from the originating organization or, if they are American National Standards, from—

American National Standards Institute

11 West 42nd Street
New York, NY 10036-8002
www.ansi.org
(212) 642-4900

Legally binding regulatory requirements are stated only in laws; NRC regulations; licenses, including technical specifications; or orders, not in NUREG-series publications. The views expressed in contractor prepared publications in this series are not necessarily those of the NRC.

The NUREG series comprises (1) technical and administrative reports and books prepared by the staff (NUREG-XXXX) or agency contractors (NUREG/CR-XXXX), (2) proceedings of conferences (NUREG/CP-XXXX), (3) reports resulting from international agreements (NUREG/IA-XXXX), (4) brochures (NUREG/BR-XXXX), and (5) compilations of legal decisions and orders of the Commission and Atomic and Safety Licensing Boards and of Directors' decisions under Section 2.206 of NRC's regulations (NUREG-0750).

DISCLAIMER: This report was prepared under an international cooperative agreement for the exchange of technical information. Neither the U.S. Government nor any agency thereof, nor any employee, makes any warranty, expressed or implied, or assumes any legal liability or responsibility for any third party's use, or the results of such use, of any information, apparatus, product or process disclosed in this publication, or represents that its use by such third party would not infringe privately owned rights.



International Agreement Report

Evaluation for 4-Inch Cold Leg Top-Slot Break LOCA in ATLAS Facility with RELAP5 Mod3.3 Patch5

Prepared by:

J. Kim*, K.-H. Kang*, B.-U. Bae*, Y. Park*, A. Shin**, M. Cho**

*Korea Atomic Energy Research Institute,
111, Daedeok-daero 989beon-gil, Yuseong-gu, Daejeon, Korea

**Korea Institute of Nuclear Safety
62 Gwahak-ro, Yuseong-gu, Daejeon 34142, Republic of Korea

K. Tien, NRC Project Manager

**Division of Systems Analysis
Office of Nuclear Regulatory Research
U.S. Nuclear Regulatory Commission
Washington, DC 20555-0001**

Manuscript Completed: February 2020

Date Published: January 2021

Prepared as part of
The Agreement on Research Participation and Technical Exchange
Under the Thermal-Hydraulic Code Applications and Maintenance Program (CAMP)

**Published by
U.S. Nuclear Regulatory Commission**

ABSTRACT

The present works, an ATLAS test for 4-Inch cold leg top-slot break LOCA and a simulation of this test with RELAP5 Mod3.3 Patch5, are presented and the calculation results are compared and discussed against the test data. An ATLAS model for RELAP5 was applied for steady state. And then, a transient calculation was performed with a break line model that was developed for the present work. The RELAP5 calculations show a reasonable agreement with the test data. Especially, the RELAP5 predicted repeatable loop seal clearing and reformation in the test. The loop seal clearing and reformation led no excursion in the cladding temperature in both the test and RELAP5 calculation.

TABLE OF CONTENTS

ABSTRACT	iii
TABLE OF CONTENTS.....	v
LIST OF FIGURES.....	vii
LIST OF TABLES.....	ix
EXECUTIVE SUMMARY	xi
ACKNOWLEDGMENTS.....	xiii
ABBREVIATIONS AND ACRONYMS.....	xv
1 INTRODUCTION.....	1
2 EVALUATION FOR 4-INCH COLD LEG TOP-SLOT BREAK IN ATLAS FACILITY.....	3
2.1 ATLAS Facility	3
2.1.1 Fluid System	3
2.1.2 Condensation Tank and Break Simulation System	7
2.1.3 Instrument and Control System.....	12
2.1.4 Uncertainty Evaluation of Measured Data	19
2.2 Major Test Results.....	19
2.2.1 Test Conditions.....	19
2.2.2 Test Procedure.....	20
2.2.3 Sequence of Events	20
2.2.4 Estimation of Heat Loss	20
2.2.5 Identified Thermal Hydraulic Phases During LTC-CL-04R.....	21
3 RELAP5 INPUT MODELS.....	37
3.1 RELAP5 Input Model for ATLAS Simulation	37
3.1.1 RELAP5 Nodalization for ATLAS Facility	37
3.1.2 Break Modeling.....	38
4 RESULTS.....	39
4.1 ATLAS Calculations and Discussions.....	39
5 RUN STATISTICS.....	49
6 CONCLUSIONS.....	51
7 REFERENCES.....	53

LIST OF FIGURES

Figure 1	Schematic Diagram of ATLAS	5
Figure 2	Isometric View of ATLAS	6
Figure 3	Arrange of Primary Loop of ATLAS for Cold Leg Break Test	7
Figure 4	Schematics of Condensation Tank.....	8
Figure 5	Drawing of Installation Scheme of Break Simulation	9
Figure 6	Drawing of Break Simulation Nozzle	10
Figure 7	ISO Drawing of Installation of Break Simulation	11
Figure 8	Measuring Location of Water Level Transmitters Installed on RPV	14
Figure 9	Measuring Location of Water Level Transmitters Installed on SG	15
Figure 10	Measuring Location of Water Level Transmitters Installed on Pressurizer.....	16
Figure 11	Cross-sectional Location of Thermocouples Installed in Core Heater Bundle	17
Figure 12	Axial Locations of Thermocouples and Spacers Installed in Core Heater Bundle	18
Figure 13	Decay Power for LTC-CL-04R Test.....	26
Figure 14	Estimated Heat Loss through System of LTC-CL-04R Test.....	26
Figure 15	Diagram of Water Level Transmitter Installation at Intermediate Leg (j: Loop index, 1A, 1B, 2A, 2B)	27
Figure 16	Water Level Behavior of LT-ILj-03 (j: Loop Index, 1A, 1B, 2A, 2B)	28
Figure 17	Water Level of Core and Downcomer of RPV.....	29
Figure 18	Core Temperatures and Saturated Temperature at Upper Head	29
Figure 19	Pressure at Pressurizer, Steam Generators and SITs.....	30
Figure 20	Condensation Tank Mass (LC-CDT-01-I) and Break Flow Rates (Triangle, Square).....	30
Figure 21	Flow Rate of SIPs and SITs.....	31
Figure 22	Flow Rate of Hot Legs	31
Figure 23	Flow Rate of Cold Legs	32
Figure 24	Location of Flow Meter of Cold Leg 1A	32
Figure 25	Differential Pressure between Downcomer and Upper Head	33
Figure 26	Thermocouple Distribution Map in Downcomer of RPV.....	33
Figure 27	Temperature of Downcomer (TF-DC-011 ~ 016).....	34
Figure 28	Temperature of Downcomer (TF-DC-021 ~ 026).....	34
Figure 29	Temperature of Downcomer (TF-DC-031 ~ 036).....	35
Figure 30	Temperature of Downcomer (TF-DC-041 ~ 046).....	35

Figure 31	Temperature of Downcomer (TF-DC-051 ~ 056).....	36
Figure 32	Temperature of Downcomer (TF-DC-061 ~ 066).....	36
Figure 33	ATLAS Nodalization of SBLOCA (or IBLOCA).....	37
Figure 34	Nodalization of Break Line	38
Figure 35	Pressurizer Pressure	39
Figure 36	Core Power	40
Figure 37	Break Flow Rate.....	40
Figure 38	Accumulated Break Flow	41
Figure 39	Core Collapsed Water Level.....	42
Figure 40	Maximum Core Temperature.....	42
Figure 41	Steam Dome Pressure of Steam Generator-1	43
Figure 42	Steam Dome Pressure of Steam Generator-2	44
Figure 43	Hot Leg-1 Flow Rate	44
Figure 44	Hot Leg-2 Flow Rate	45
Figure 45	Collapsed Water Level at Vertical Intermediate Leg (Exp.)	46
Figure 46	Collapsed Water Level at Vertical Intermediate Leg (RELAP5)	47

LIST OF TABLES

Table 1	Major Scaling Parameters of ALTAS	4
Table 2	Summary of ATLAS Instrument Channels	13
Table 3	Uncertainty Levels of Instruments.....	19
Table 4	Control Logic Setting for LTC-CL-04R Test.....	23
Table 5	Actual Initial and Boundary Condition for LTC-CL-04R Test.....	24
Table 6	Actual Sequence of Events of LTC-CL-04R Test.....	25
Table 7	Run Statistics.....	49

EXECUTIVE SUMMARY

The present works, an ATLAS test for 4-Inch cold leg top-slot break LOCA [1] and a simulation of this test with RELAP5 Mod3.3 Patch5 are presented. The test was performed to resolve an issue about the effect of loop seal clearing and reformation on a peak cladding temperature during a cold leg top-slot break LOCA for APR1400. The calculation results are compared against the test data and the major thermal-hydraulic behaviors were discussed in both the test and calculation focused on loop seal clearing and reformation. An ATLAS model for RELAP5 was applied for steady state. And then, a transient calculation was performed with a break line model that was developed for the present works.

The RELAP5 calculations show a reasonable agreement with the test data. Especially, the RELAP5 predicted repeatable loop seal clearing and reformation in the test. The loop seal clearing and reformation led no excursion in the cladding temperature in both the test and RELAP5 calculation. There are some discrepancies in the prediction of the secondary system pressure. The reason for these discrepancies could be attributed to non-application of a heat loss model to the secondary system of a steam generator. In terms of the overall trend for loop seal behavior, the calculation shows a good agreement with the ATLAS data, but a detailed timing of loop seal clearing and reformation shows a discrepancy between the test and the calculation.

ACKNOWLEDGMENTS

This work was supported by a National Research Foundation of Korea (NRF) grant funded by the Korean government (Ministry of Science and ICT) (NRF-2017M2A8A4015026).

ABBREVIATIONS AND ACRONYMS

AFW	Auxiliary Feed Water
APR1400	Advanced Power Reactor 1400 MWe
ASME	American Society of Mechanical Engineers
ATLAS	Advanced Thermal- hydraulic Test Loop for Accident Simulation
BDFT	Bi-Directional Flow Tube
CDT	Condensation Tank
CL	Cold Leg
DC	Downcomer
DCS	Distributed Control System
DVI	Direct Vessel Injection
ECC	Emergency Core Cooling
EU	Engineering Units
FLB	Feed Line Break
HL	Hot Leg
HMI	Human Machine Interface
HPSI	High Pressure Safety Injection
IL	Intermediate Leg
KAERI	Korea Atomic Energy Research Institute
LBLOCA	Large Break Loss of Coolant Accident
LOCA	Loss of Coolant Accident
LPP	Low Pressurizer Pressure
LUDP	Low Upper Downcomer Pressure
IBLOCA	Intermediate Break Loss of Coolant Accident
MFIV	Main Feedwater Isolation Valve
MSIV	Main Steam Isolation Valve
MSSV	Main Steam Safety Valve
OPR1000	Optimized Power Reactor 1000 MWe
PZR	Pressurizer
RCP	Reactor Coolant Pump
RPV	Reactor Pressure Vessel
RWT	Refueling Water Tank

SBLOCA	Small Break Loss of Coolant Accident
SG	Steam Generator
SGSD	Steam Generator Steam Dome
SGTR	Steam Generator Tube Rupture
SIP	Safety Injection Pump
SIT	Safety Injection Tank
UH	Upper Head

1 INTRODUCTION

In the present works, an ATLAS test for 4-Inch cold leg top-slot break LOCA (Ref.1) and a simulation of this test with RELAP5 Mod3.3 Patch5 are presented and the calculation results are compared against the test data.

The test was performed to resolve an issue about the effect of loop seal clearing and reformation on the peak cladding temperature during a cold leg top-slot break LOCA for APR1400. For a short time period of reflood, the ECCS of APR1400 must be capable of providing long term decay heat removal for up to 30 days. During a postulated design basis cold leg slot break, the ECCS design must also provide decay heat removal to prevent the core from being uncovered. With a reactor coolant pump suction side loop seal elevation close to the midpoint of the core height, the steam pressure in the upper part of the core may increase to the point of overcoming the static head of the loop seal. APR1400 design was required to provide the technical basis to show that the reactor core cooling will be maintained before and after the potential loop seal clearing and that the peak cladding temperature remains within acceptable limits.

The assessment of RELAP5 Mod3.3 Patch5 was performed in the present ATLAS test. An ATLAS model for RELAP5 was applied for steady state. And then, a transient calculation was performed with a break line model that was developed for the present work. The calculation results are compared against the test data and the major thermal-hydraulic behaviors were discussed in both the test and calculation focused on loop seal clearing and reformation.

2 EVALUATION FOR 4-INCH COLD LEG TOP-SLOT BREAK IN ATLAS FACILITY

2.1 ATLAS Facility

2.1.1 Fluid System

ATLAS is a thermal-hydraulic integral effect test facility for evolutionary pressurized water reactors of APR1400 and OPR1000. The reference plant of ATLAS is APR1400, which is an advanced power reactor developed by the Korean nuclear industry and has a rated thermal power of 4000 MW and a loop arrangement of 2 hot legs and 4 cold legs for the reactor coolant system (Ref. 2). ATLAS also incorporates some specific design features of the Korean standard nuclear power plant, OPR1000, such as a cold-leg injection and a low-pressure safety injection mode for emergency core cooling. ATLAS can be used to investigate multiple responses between the systems for a whole plant or between the subcomponents in a specific system during anticipated transients and postulated accidents.

ATLAS has the same two-loop features as APR1400 and was designed according to a well-known scaling method suggested by Ishii and Kataoka (Ref. 3 and 4) to simulate various test scenarios as realistically as possible. It is a half-height and 1/288-volume scaled test facility with respect to a reference plant of APR1400. The main motive for adopting a reduced-height design is to allow for an integrated annular downcomer where the multidimensional phenomena can be important in some accident conditions with a DVI operation. According to the scaling law, the reduced height scaling has the time-reducing results in the model. For the one-half-height facility, the time for the scaled model is 1.4 times faster than the prototypical time. The friction factors in the scaled model are maintained the same as those of the prototype. The hydraulic diameter of the scaled model is maintained the same as that of the prototype to preserve the prototypical conditions for the heat transfer coefficient. Major scaling parameters of ATLAS are summarized in Table 1.

The fluid system of ATLAS consists of a primary system, a secondary system, a safety injection system, a break simulating system, a containment simulating system, and auxiliary systems. The primary system includes a reactor pressure vessel, two hot legs, four cold legs, a pressurizer, four reactor coolant pumps, and two steam generators. The secondary system of ATLAS is simplified to be of a circulating loop-type. The steam generated at two steam generators is condensed in a direct condenser tank and the condensed feedwater is again injected to the steam generators. Most of the safety injection features of APR1400 and OPR1000 are incorporated into the safety injection system of ATLAS. It consists of four safety injection tanks (SITs), a high-pressure safety injection pump (SIP) which can simulate safety injection and long-term cooling, a charging pump for charging an auxiliary spray, and a shutdown cooling pump and a shutdown heat exchanger for low pressure safety injection, shutdown cooling operation and recirculation operation. The break simulation system consists of several break simulating lines such as LBLOCA, DVI line break LOCA, SBLOCA, SGTR, MSLB, and FLB, etc. Each break simulating line consists of a quick opening valve, a break nozzle and instruments. It is precisely manufactured to have a scaled break flow through it in the case of LOCA tests. The containment simulating system of ATLAS has a function of collecting the break flow rate and maintaining a specified back-pressure in order to simulate containment. Besides,

ATLAS has some auxiliary systems such as a makeup system, a component cooling system, a nitrogen/air/steam supply system, a vacuum system, and a heat tracing system.

A schematic diagram of ATLAS is shown in Figure 1. More realistic 3-dimensional view of ATLAS is shown in Figure 2, including a reactor pressure vessel, two steam generators, four reactor coolant pumps, a pressurizer, and four safety injection tanks. A system arrangement and labeling of the primary loop for the cold leg SBLOCA test can be observed in Figure 3. Detailed design and description of the ATLAS facility can be found in Ref. 5. The condensation and break simulation systems in ATLAS are described in the following sections.

Table 1 Major Scaling Parameters of ALTAS

Parameters	Scaling law	ATLAS design
Length	l_{OR}	1/2
Diameter	d_{OR}	1/12
Area	d_{OR}^2	1/144
Volume	$l_{OR} d_{OR}^2$	1/288
Core DT	ΔT_{OR}	1
Velocity	$l_{OR}^{1/2}$	$1/\sqrt{2}$
Time	$l_{OR}^{1/2}$	$1/\sqrt{2}$
Power/Volume	$l_{OR}^{-1/2}$	$\sqrt{2}$
Heat flux	$l_{OR}^{-1/2}$	$\sqrt{2}$
Core power	$l_{OR}^{1/2} d_{OR}^2$	1/203.6
Flow rate	$l_{OR}^{1/2} d_{OR}^2$	1/203.6
Pressure drop	l_{OR}	1/2

where, l is length, d is diameter, and T is temperature.

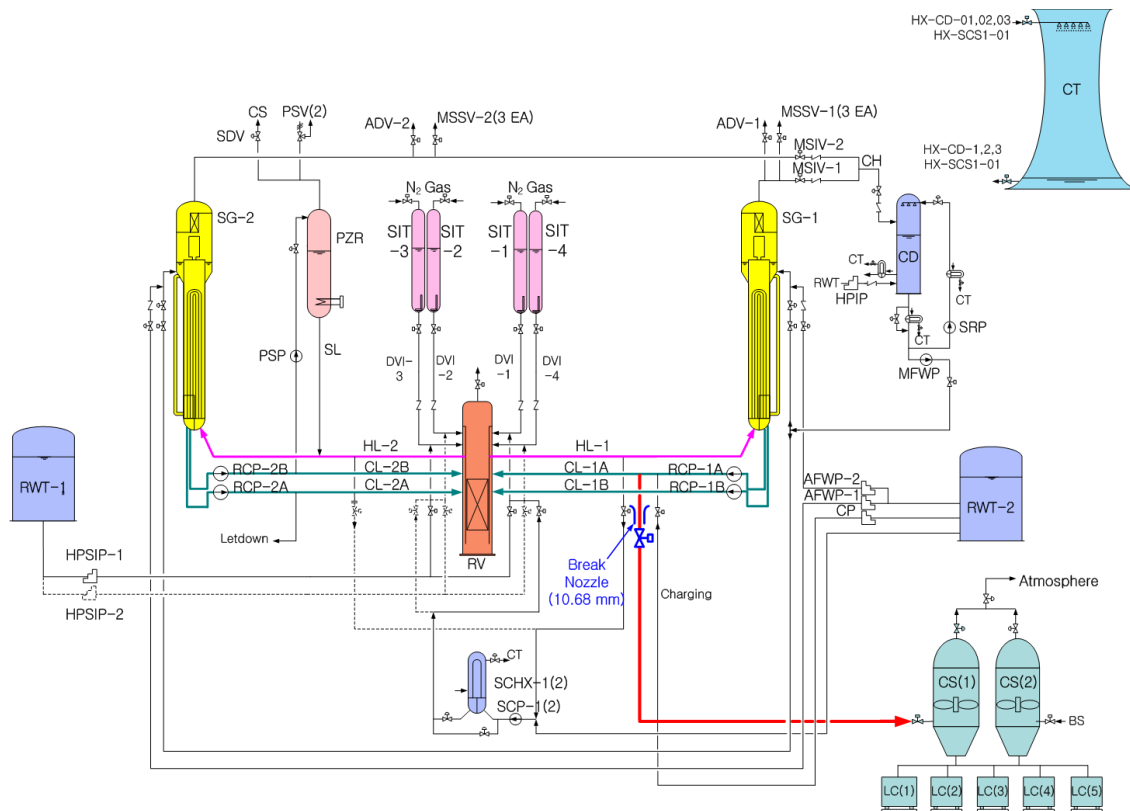


Figure 1 Schematic Diagram of ATLAS

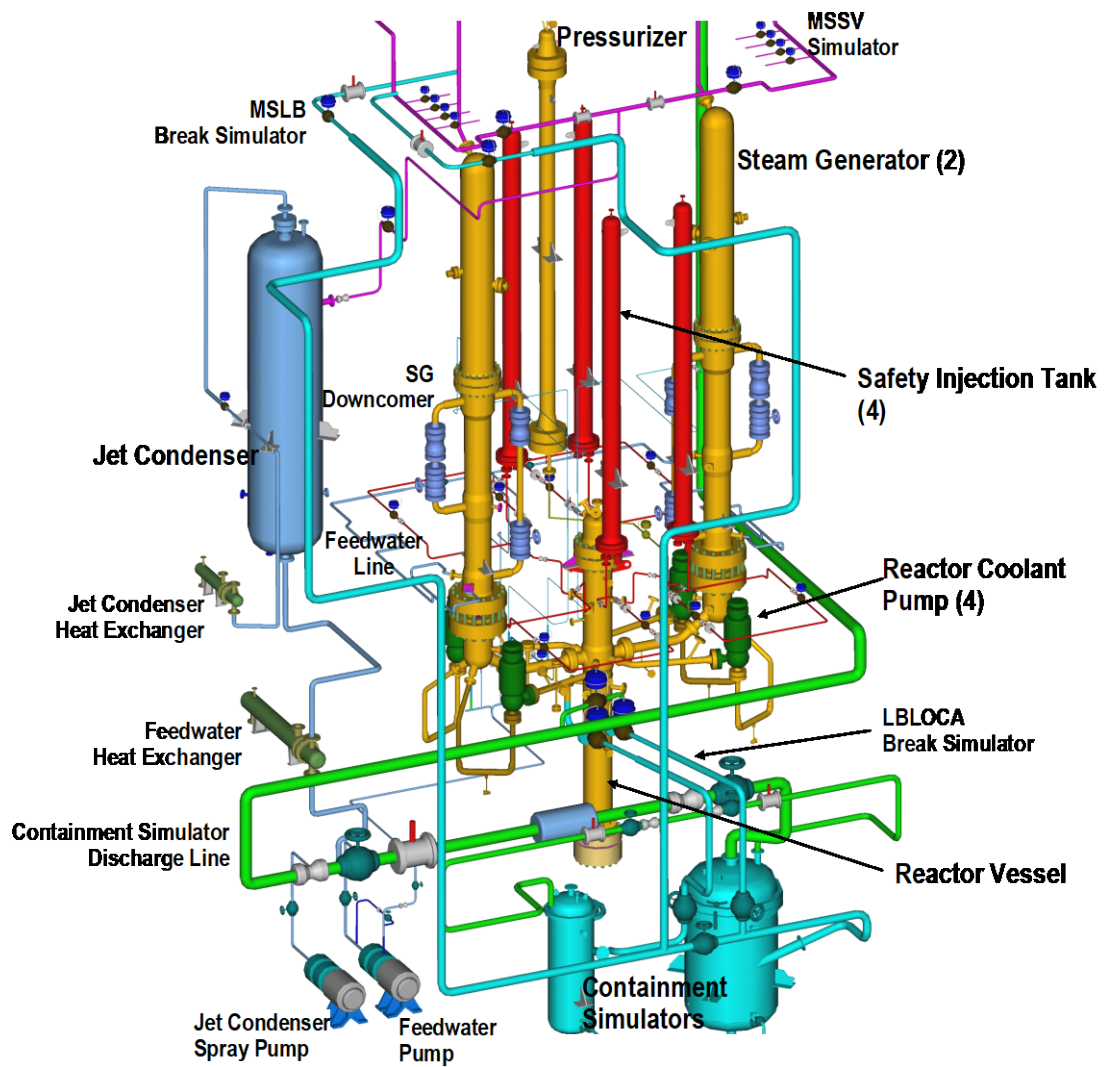


Figure 2 Isometric View of ATLAS

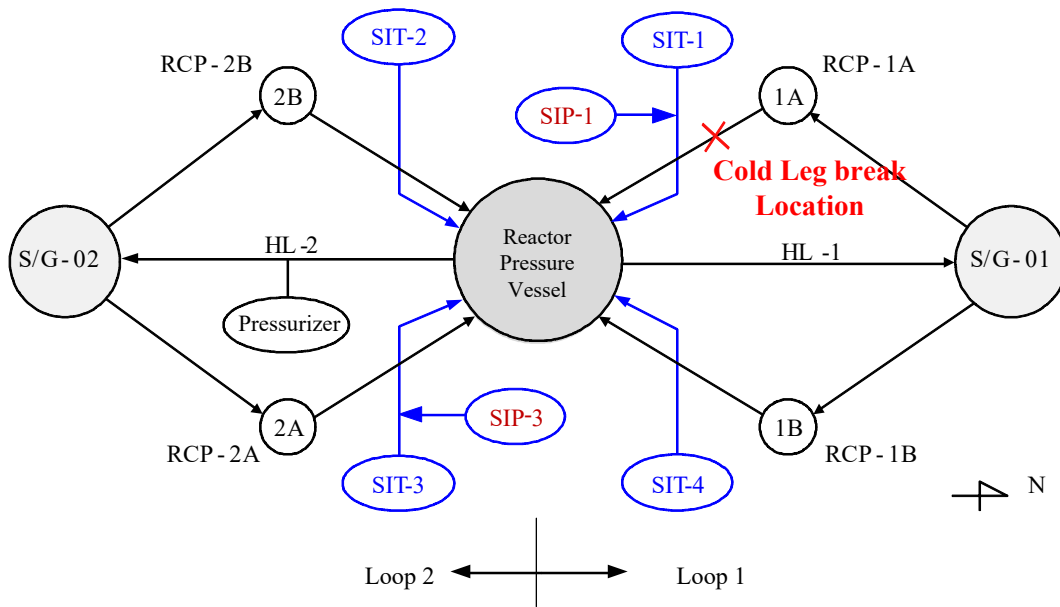


Figure 3 Arrange of Primary Loop of ATLAS for Cold Leg Break Test

2.1.2 Condensation Tank and Break Simulation System

The break flow is discharged to a condensation tank, which consists of a sparger and a measuring tank. Overall configuration of the condensation tank is shown in Figure 4. Discharged steam and water flow into the sparger in the condensation tank and then steam is directly condensed in the tank. Drained water and condensed steam are measured by the load cells and the break flow is calculated by the mass increasing rate of load cells.

A break simulator consists of a quick opening valve (OV-CLBS-01), a break nozzle and its housing, and related instruments. Detailed geometry of the break nozzle and the break line from the cold leg to the condensation tank for the present test can be observed from Figure 5 to Figure 7, respectively. The break line was installed at the top of the cold leg pipe to simulate a top slot break. The inner diameter of the break nozzle was determined to be 7.12 mm which corresponds to 1/203.6 of a 4 inch break area. The break nozzle has a well-rounded entrance and the total length is up to 110 mm including the entrance region to comply with the long pipe requirement that the length to diameter ratio should be above 12 and the length should be longer than 100 mm. Before the test, the pipe line from the cold leg to the opening valve was filled with water.

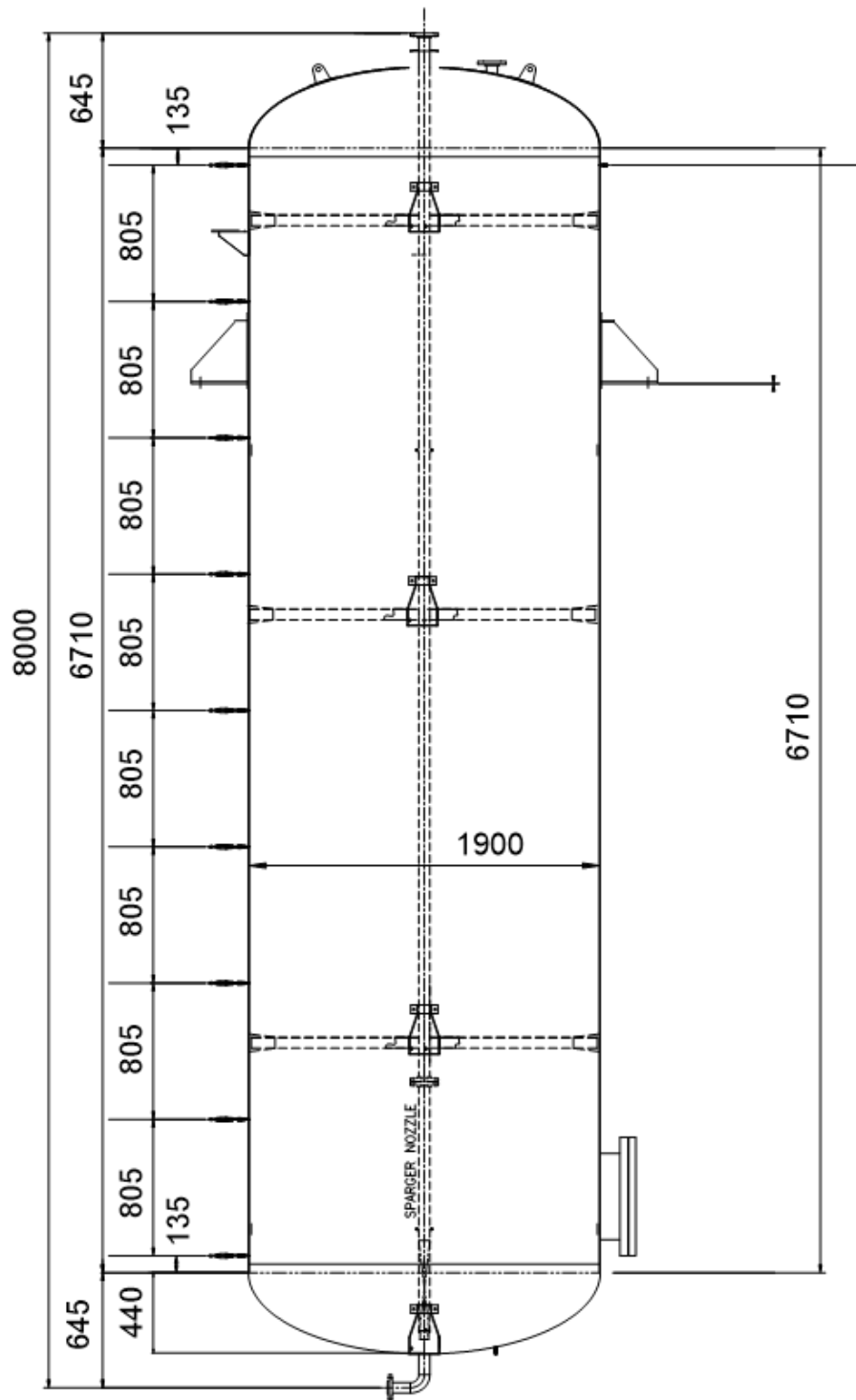


Figure 4 Schematics of Condensation Tank

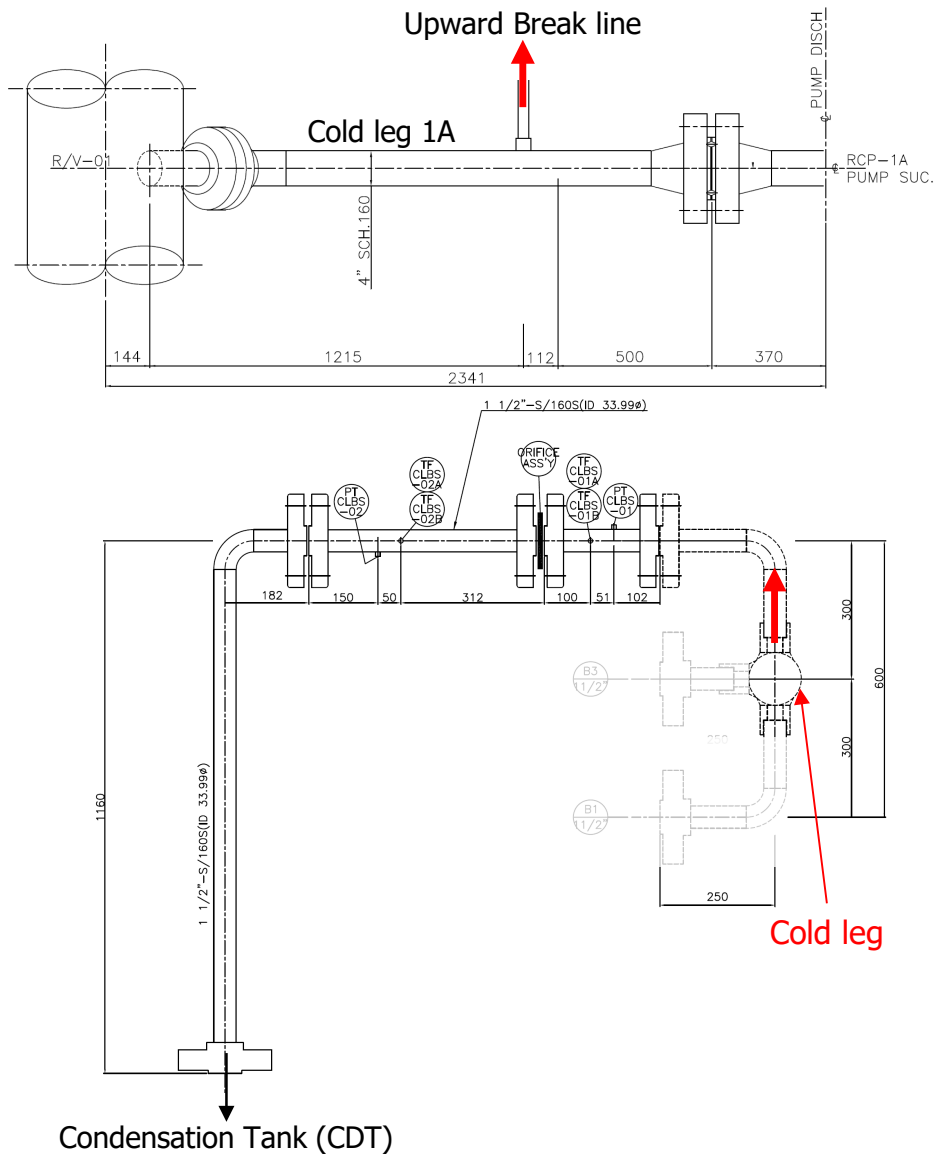


Figure 5 Drawing of Installation Scheme of Break Simulation

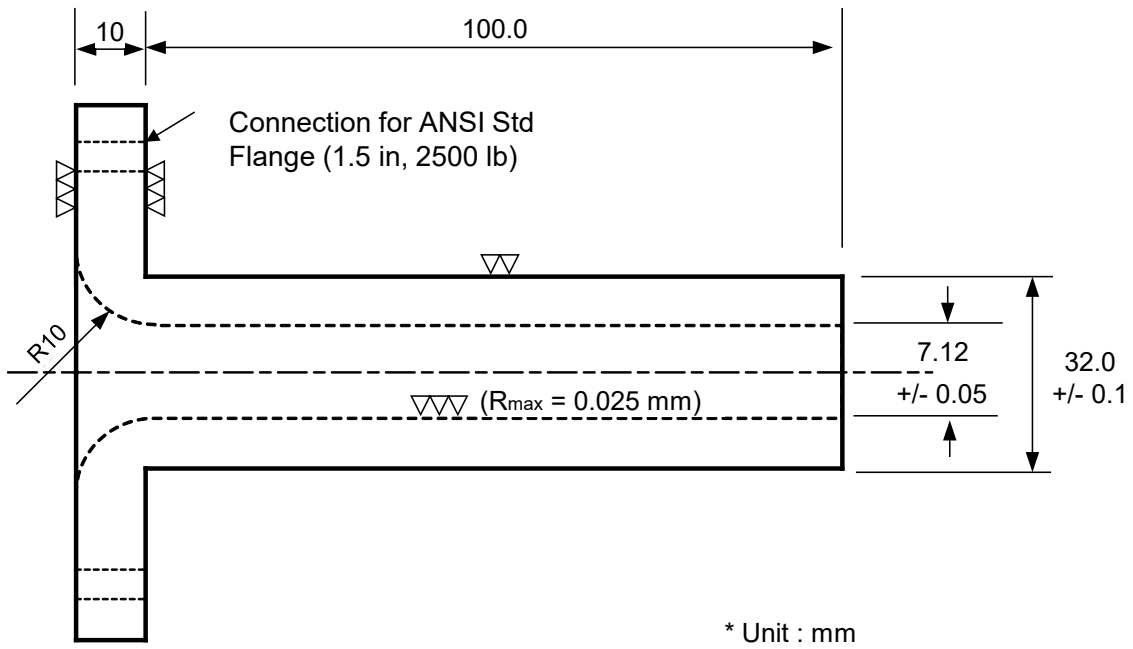


Figure 6 Drawing of Break Simulation Nozzle

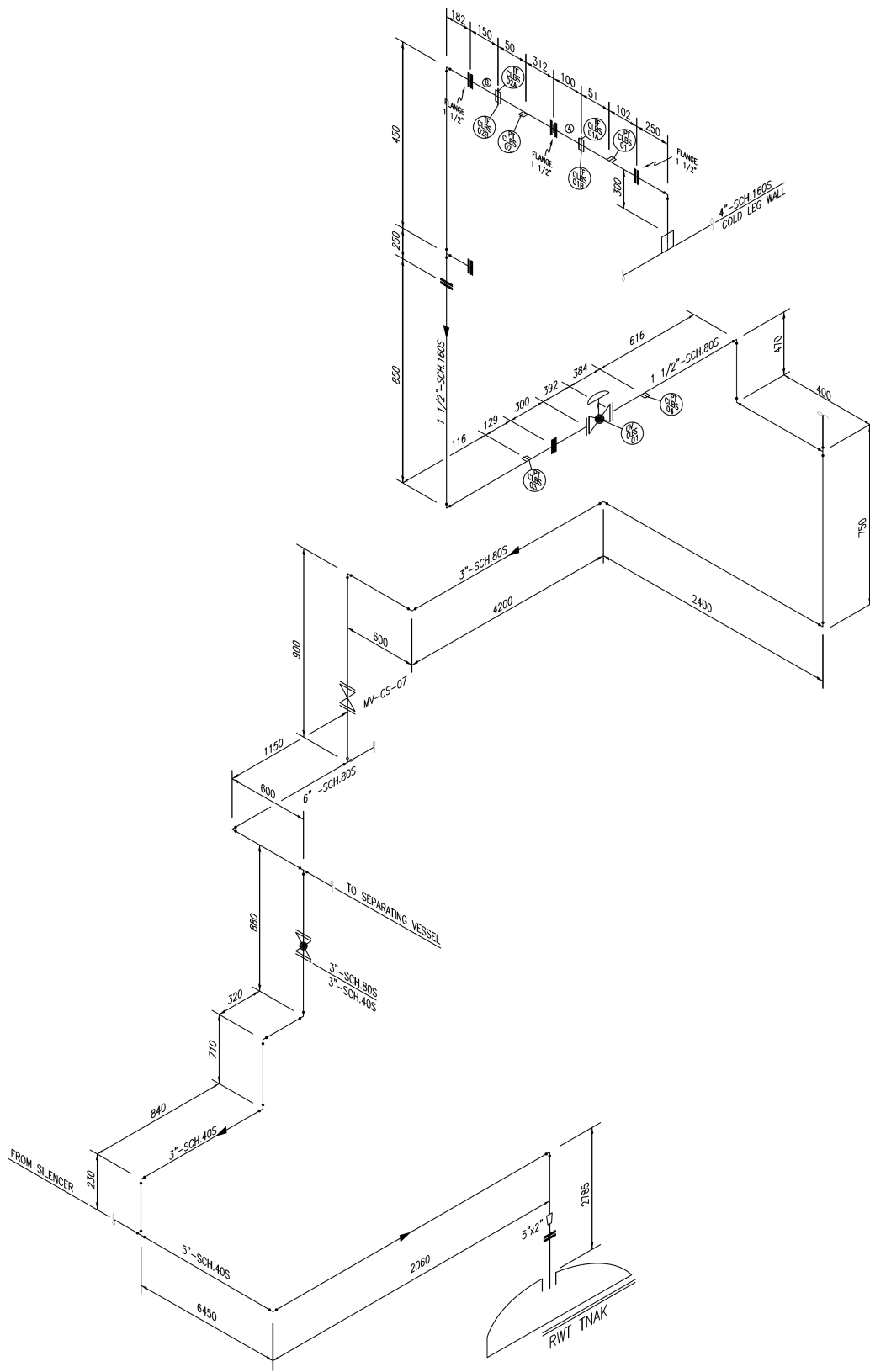


Figure 7 ISO Drawing of Installation of Break Simulation

2.1.3 Instrument and Control System

The control and data acquisition system of ATLAS has been built with a hybrid distributed control system (DCS). The input and output modules are distributed in 10 cabinets and they are controlled by two CPUs. Raw signals from the field are processed or converted to engineering units (EU) in a system server and the processed or converted signals are monitored and controlled through the Human Machine Interface (HMI) system by operators.

Instrumentation signals of ATLAS consist of measurement-based analog input signals and control-based in-out signals such as Analog Input (AI), Analog Output (AO), Thermocouple (TC), Digital Input (DI), Digital Output (DO), and Serial communication (SR). The number of instruments is about 1,600 at present, and the number of each signal-processing group can be identified in Table 2. Instrument signals can also be categorized according to the instrument type such as temperature, static pressure, differential pressure, water level, flow rate, power, and rotational speed. The locations of the instruments for measuring the water levels of a reactor pressure vessel, a steam generator, and a pressurizer are shown in Figure 8 through Figure 10, respectively. There are 390 electric heaters which are divided concentrically into 3 groups (Group-1, Group-2 and Group-3). Group-1, -2, and -3 heaters are located in inner, middle, and outer regions of the heater bundle, respectively, and they have 102, 138 and 150 heaters, respectively. The cross-sectional locations of the thermocouples installed in the core heater bundles are shown in Figure 11 and the axial locations of the thermocouples, spacer grids, and level transmitters are shown in Figure 12.

The data logging system can be started or stopped by operators and a logging frequency can be selected from among 0.5, 1, 2, 10 Hz. In the present test, the logging frequency was 1 Hz. In the ATLAS test facility, about 1,600 instruments are installed for the measurement of thermal hydraulics phenomena in the components. Most of the instruments are chosen from commercially available ones. However, an average bi-directional flow tube (BDFT or BiFlow) and a break flow system were specially developed or designed for the measurements of the flow rates in the primary piping and in the containment system, respectively.

Table 2 Summary of ATLAS Instrument Channels

	Temperature					Pressure			Flow			Etc.					Total
	TH	TF	TW	TI	TA	PT	DP	LT	QV	QM	BDFT	LC	EP	TR	RS	VF	
RPV	262	90	38	4	2	3	5	26					3				433
Loop		72	56	20		6	23	18			12		4		4		215
SG		124	92	6	2	6	2	36	4								272
PZR	2	11	13	3		2	1	9	1				2				44
2nd sys.		24				12		1	12								49
SDS		2				1											3
SIS	4	36	8			26		6	14								94
CS		13				5			3	1		5					27
CWS		6				1			2								9
SSS		1				2											3
MWS		1				1		1									3
NSS		1				2			1								4
Spool		28				20	2		2								52
CAS						1											1
Trace													25				25
VAS						1		1									2
Total	268	409	207	33	4	89	33	98	39	1	12	5	34	0	4	0	1236
	921						220	52									

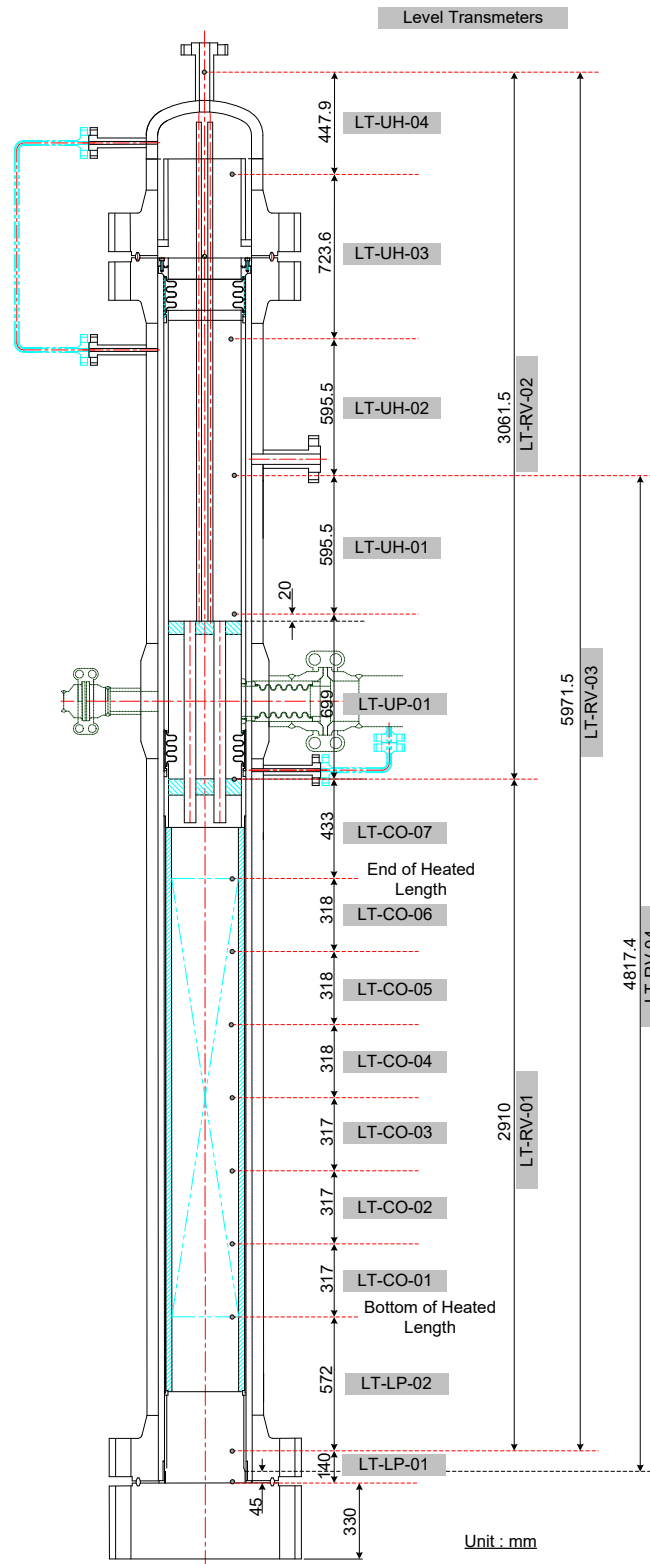


Figure 8 Measuring Location of Water Level Transmitters Installed on RPV

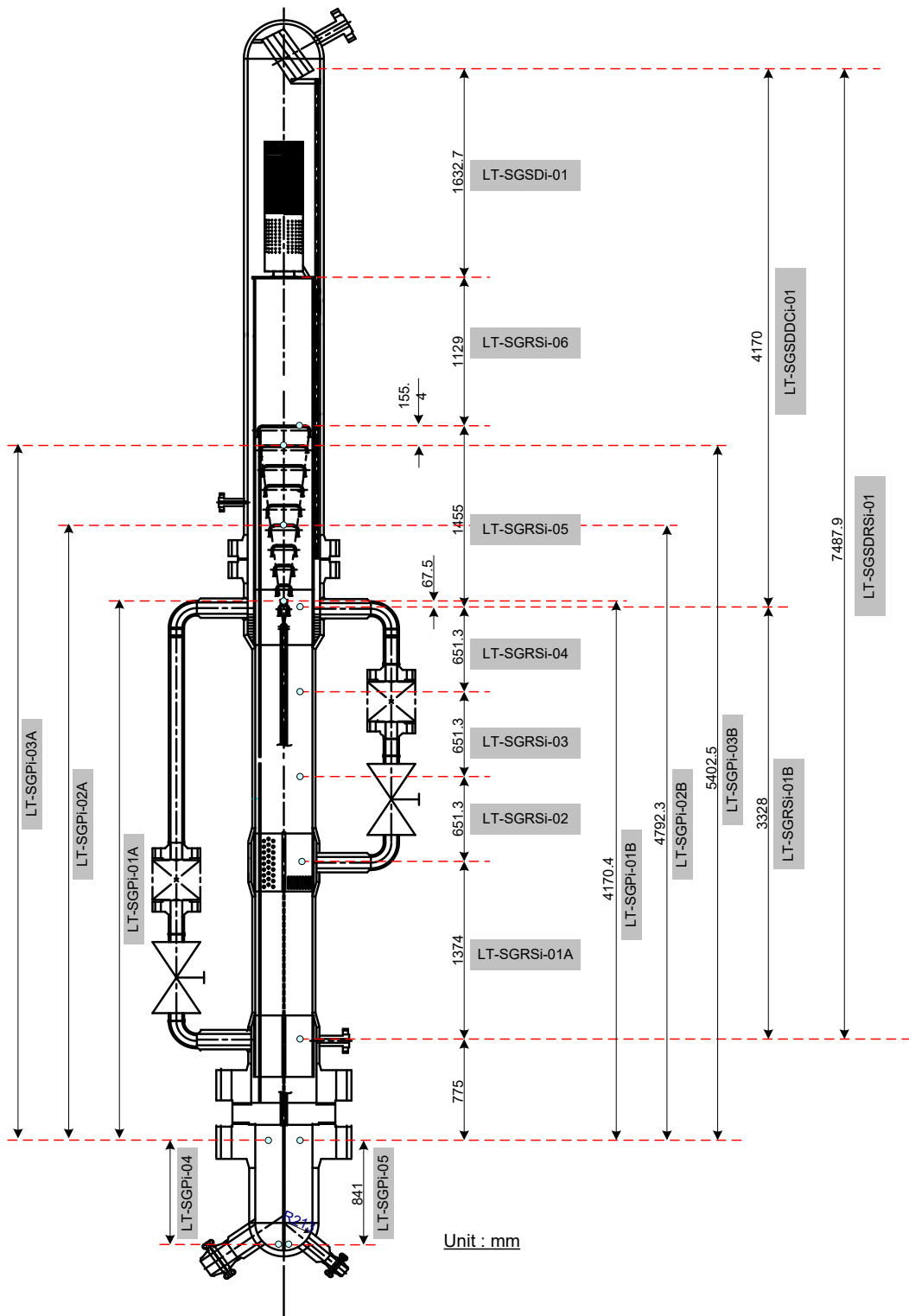


Figure 9 Measuring Location of Water Level Transmitters Installed on SG

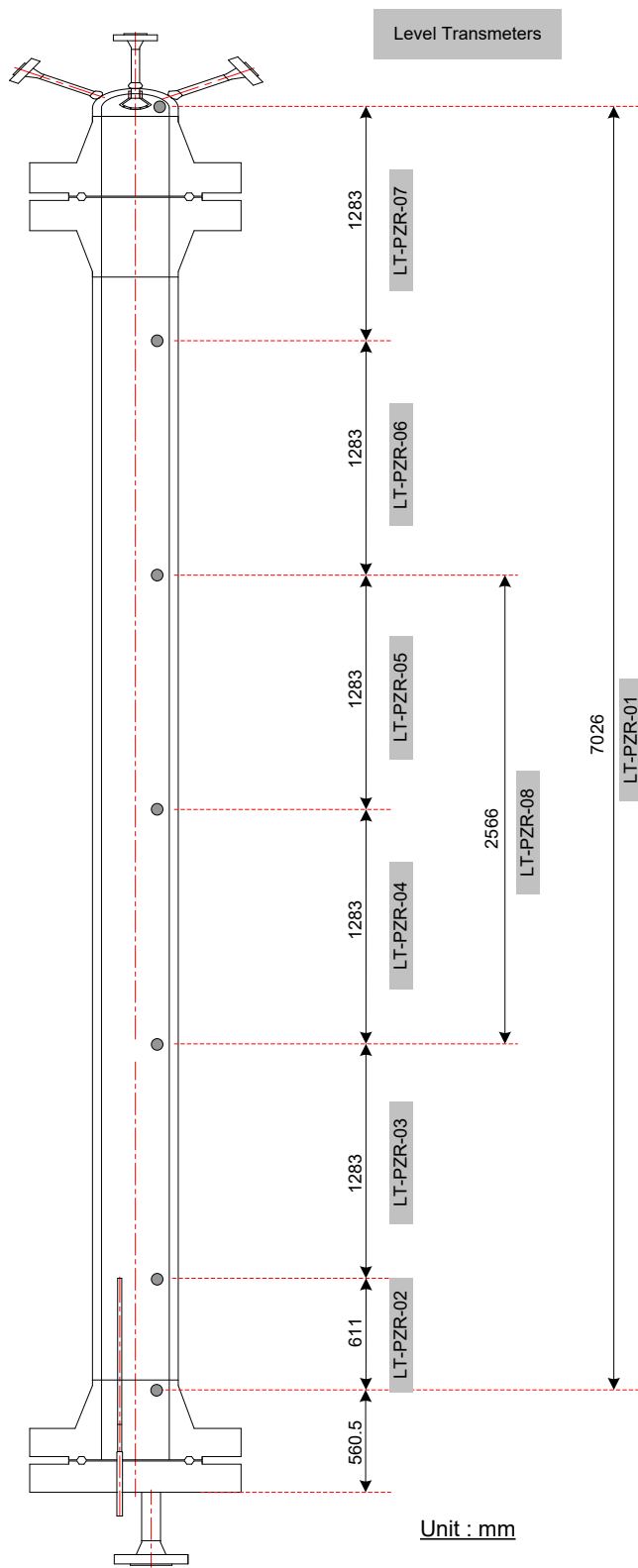


Figure 10 Measuring Location of Water Level Transmitters Installed on Pressurizer

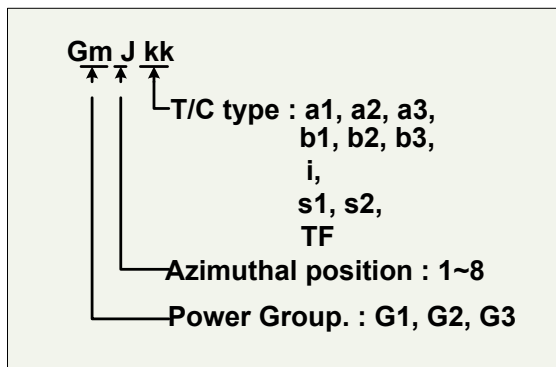
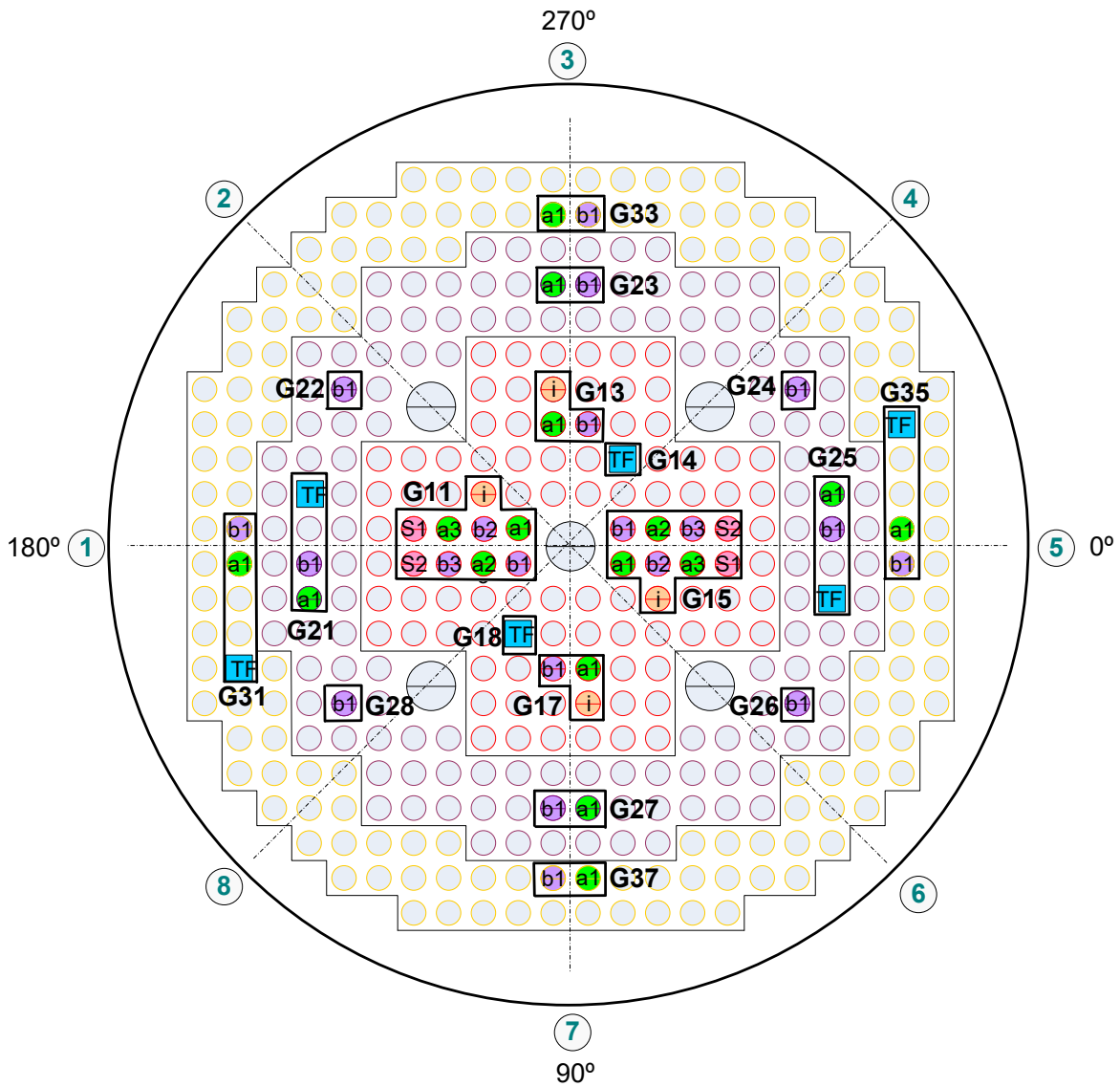


Figure 11 Cross-sectional Location of Thermocouples Installed in Core Heater Bundle

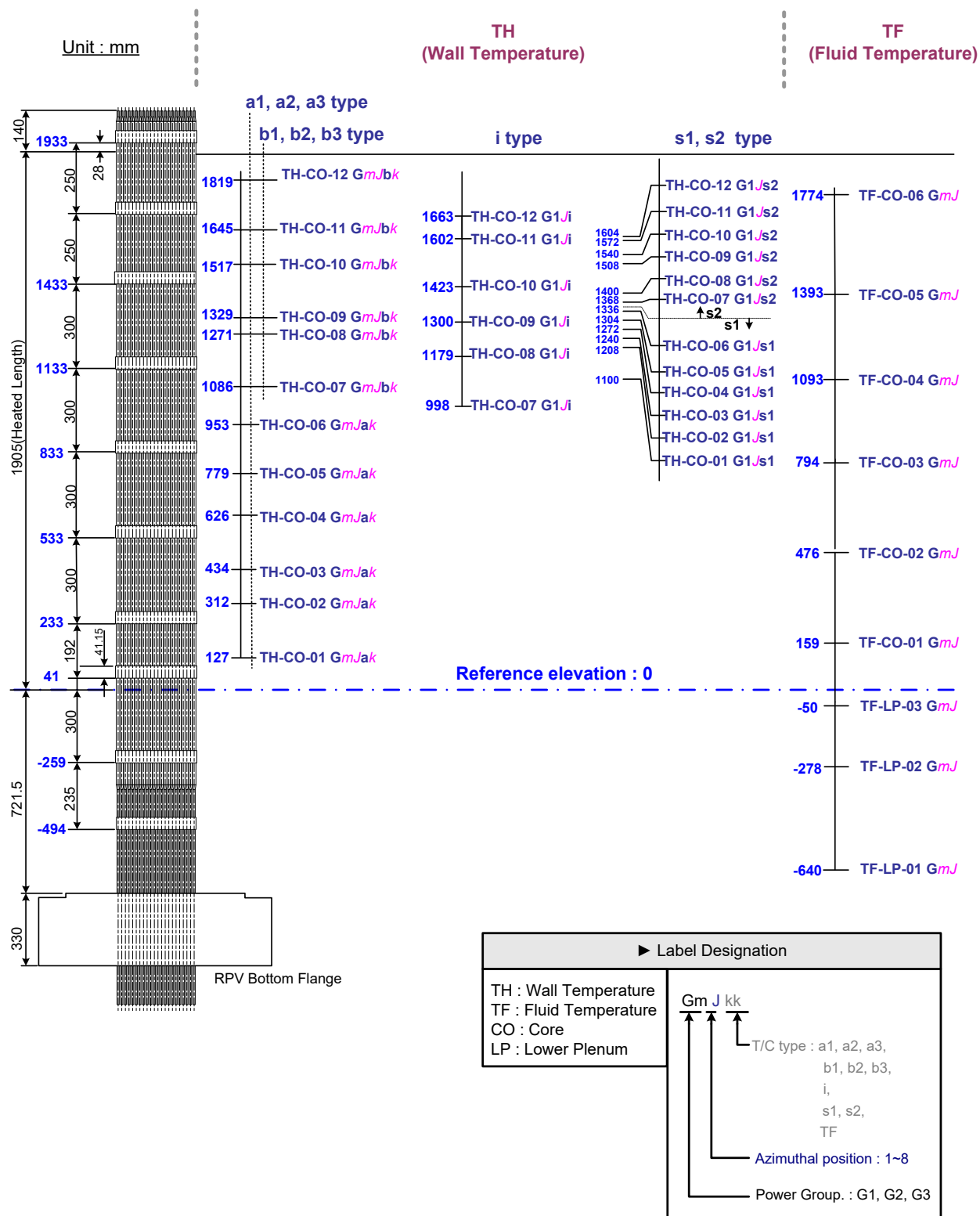


Figure 12 Axial Locations of Thermocouples and Spacers Installed in Core Heater Bundle

2.1.4 Uncertainty Evaluation of Measured Data

Uncertainty of the measured test data was analyzed in accordance with a 95% confidence level. According to the ASME performance test codes 19.1, the uncertainty interval of the present results was given by the root-mean-square of a bias contribution and a precision contribution. The bias and precision errors were evaluated from the data acquisition hardware specifications and the calibration results performed once every year, respectively. Table 3 shows analyzed uncertainty levels of each group of instruments.

Table 3 Uncertainty Levels of Instruments

Items	Unit	Uncertainty
Static Pressure	MPa	0.039
Differential Pressure	kPa	0.23
Collapsed Water Level	%	0.18 (Core) 2.6 (Downcomer) 8.6 (RCP suction side of the intermediate leg)
Temperature	°C	maximum 2.4
Flow rate	kg/s	0.053
Loop flow rate	%	15 (two-phase flow) 13 (liquid-phase flow)
Break flow	kg/s	0.07 (by the load cell-based measuring) by the RCS inventory change)

2.2 Major Test Results

ATLAS test, named LTC-CL-04R, was performed to investigate the effect of loop seal clearing and reformation on coolability of APR1400 during a 4-inch cold leg top-slot break LOCA transient.

2.2.1 Test Conditions

In the present test, four SITs and four SIPs were utilized as a safety injection system during the test period, and operation of the MSSVs and supply of the auxiliary feedwater were assumed to be available. The initial and boundary conditions were obtained by applying the scaling ratios, shown in Table 1.

A set of characterization tests was performed for reliable simulation of the scaled-down safety injection flow rates by the SIPs. In the present test, the maximum SIP flow rate and relatively cold ECC water temperature were assumed to promote repeatable loop seal clearing and reformation. The estimated maximum SIP flow rate of APR1400 was about 65.2 kg/s and thus,

according to the scaling ratio, 0.32 kg/s of ECC water should be delivered to the reactor pressure vessel through the each DVI nozzle. In the ATLAS facility, the ECC water was supplied from the RWT and the temperature of around 10 to 17 °C was in the operating range as that of APR1400. The SIP flow rate was dependent on the pressure difference between the SIT and the primary system.

The decay heat was simulated to be 1.2 times of the ANS-73 decay curve for the conservative condition. The initial heater power was controlled to maintain at 1.64 MW, which is equal to the sum of the scaled-down core power (1.567 MW) and the heat loss rate of the primary system (about 88 kW), and then the heater power was controlled to follow the specified decay curve after 31.7 seconds from the opening of the break valve as shown in Figure 13. There are four bypass valves connected to the downcomer in ATLAS. Two bypass valves of FCV-RV-37 and FCV-RV-38 are between the downcomer and the upper head, and two bypass valves of FCV-RV-95 and FCV-RV-96 are between the downcomer and hot legs. All bypass valves were closed to provide a conservative condition for loop seal clearing and reformation. In Table 4, the major control logics are summarized. In Table 5, the actual initial and boundary conditions of the LTC-CL-04R test can be observed.

2.2.2 Test Procedure

Prior to a transient test, several actions were taken. They included an instrument calibration with the ATLAS system drained, purging and filling the ATLAS system including leakage tests, an instrument calibration with the water-filled primary system, and an implementation of test specific control logics into the process control computers for sequence control. The sequence control logics executed the required control actions for the corresponding control devices such as the main core heater, RCP, SIP, and valves.

The whole system reaching a specified initial condition for the test as shown in Table 6, the steady-state conditions of the primary and secondary systems were maintained for more than 30 minutes. After this steady-state period, the main test started by opening of the break simulation valve, OV-CLBS-01.

2.2.3 Sequence of Events

After opening the break simulation valve, OV-CLBS-01, the test sequence was controlled by the corresponding control logic, which defined the set-point and related time delay as can be observed in Table 4. When the pressurizer pressure measured by PT-PZR-01 decreased below 10.7 MPa, the LPP signal was issued. After the LPP signal, the reactor, RCP, and pressurizer heater were tripped with no time delay. The main feed water isolation valves were closed with the LPP signal. The actuation of the SIPs was set to occur with 28 seconds delay from the LPP signal. Further decreasing of the primary pressure, below 4.03 MPa (the low upper downcomer pressure, LUDP), resulted in passive injection of the SIT water. Table 6 shows the actual progress of the events observed in the present LTC-CL-04R test.

2.2.4 Estimation of Heat Loss

The heat loss from the primary system to the environment cannot be completely prevented even though thick insulation materials envelop the reactor pressure vessel and the primary pipelines. The heat loss was estimated by the following simplified empirical correlation;

$$Q_{loss,1} = 0.32 \cdot (T_w - T_{atm}) \quad (3.4.1)$$

where T_w is outer wall surface temperature measured at the middle of the reactor pressure vessel, TW-DC-04A and T_{atm} is atmospheric temperature measured on the test day.

The heat loss from each steam generator to the environment was also estimated according to the following empirical correlation;

$$Q_{loss,2} = 0.00077 \cdot (T_w - T_{atm})^{1.8843} \quad (3.4.2)$$

where T_w is averaged values of the temperatures measured at the outer wall surface of the steam generators, TW-SGP1-02A, TW-SGRS1-01A, TW-SGRS1-02A, TW-SGRS1-03A, TW-SGSD1-01A, TW-SGSD1-02A and T_{atm} is atmospheric temperature.

Estimated heat losses through the primary and the secondary systems were about 88 kW and 33 kW, respectively. The estimated heat loss through the system can be observed in Figure 14.

2.2.5 Identified Thermal Hydraulic Phases During LTC-CL-04R

Loop seal clearing and reformation are recognized with the water level of the intermediate leg (IL) of the primary loop. Figure 15 shows the installation position of the water level transmitter at the intermediate leg. For the loop seal clearing, LT-ILj-03 became lower than the top of the horizontal intermediate leg. In other hand, LT-ILj-03 became higher than the top of the horizontal intermediate leg for the loop seal reformation. Figure 16 shows the water level behavior measured by LT-ILj-03.

Figure 17 shows the water level of the core and the downcomer. The LTC-CL-04R test was finished when the core water level recovered the elevation of hot legs and cold legs. During the loop seal clearing, the coolant at the intermediate leg flowed to the core and the core water level increased. After the loop seal reformation, the accumulated steam that was produced by decay heat increased the upper head pressure and the increased pressure pushed down the core water level.

Figure 18 shows the core temperatures and saturated temperature at the upper head. After the loop seal reformation, the core temperatures slowly increased. A reason for this increase can be attributed to the accumulated steam at the upper head that increased the pressure and saturated temperatures. Therefore, this temperature behavior was not a critical phenomenon that affected the overall coolability of the reactor coolant system during the transient.

Figure 19 shows the pressure behavior of pressurizer, steam generators, and SITs. The pressure of pressurizer (PT-PZR-01-I) generally decreased during the test period and some peaks were observed at the timing of loop seal clearing and reformation. The pressure of SITs (PT-SIT1/2/3/4-02-I) decreased along the pressure of pressurizer after SIT valve opening. The pressure of steam generators (PT-SGSD1-01-I, PT-SGSD2-01-I) increased after isolation of the feed and steam lines and MSSVs started to be operated. After then, the pressure of steam generators gradually decreased by heat transfer from the secondary side to the primary side at

steam generators because the saturation temperatures of the primary system were lower than those of the secondary system.

In Figure 20, the mass of inventory measured at the condensation tank (LC-CDT-01-I) and the break flow rate were plotted. The condensation tank mass decreased during 4500 to 5500 seconds when corresponded to the drainage time of the condensation tank because the accumulated mass of break flow at that time was beyond the capacity of the condensation tank. There are two break flow rate curves – the black triangle and the red square in Figure 20. The black triangle curve is a break flow rate that was estimated from the change of the coolant mass inventory at the primary loop. The red square curve is a break flow rate that was calculated from the change of the inventory mass in the condensation tank. The break flow by mass inventory has an empty period due to the drainage time of the condensation tank. The break flow rates were calculated using differential value of mass data. The original break flow data included noise data by calculation. To reduce the calculation noise, 20 points moving averaged data was presented in Figure 20. Before the operation of SIT, the break flow was relatively higher than that after the operation of SIT since initially the water was discharged through the break. After the operation of SIT, the break flow rate became similar with the safety injection flow rate as shown in Figure 21.

Figure 22 and Figure 23 show the flow rate of hot legs and cold legs → legs, respectively. The flow rate of cold leg 1A was negative value after the break because the flow meter was located between the RPV and the break line as shown in Figure 24. For a normal operating condition, the coolant in a cold leg flows from a steam generator to a RPV. In the case of LTC-CL-04R test, however, flow direction at flow meter of cold leg 1A was opposite because the coolant flowed out through the break line from both the RPV and the steam generator.

Differential pressures between the downcomer and the upper head of a RPV are shown in Figure 25. From this graph, an inverse flow direction can be recognized. Figure 26 shows a thermocouple distribution map in the downcomer of a RPV and Figure 27 to Figure 32 show the fluid temperatures measured at the downcomer of a RPV. The fluid temperatures adjacent to the lower plenum were relatively high, but there was no significant difference for the azimuthal direction.

Table 4 Control Logic Setting for LTC-CL-04R Test

	Set point
Primary logic	
By-pass rate	0 %
Cold leg break	300 sec
LPP	PT-PZR-01 < 12.48MPa
Reactor scram / TCP trip / RCP trip/ Turbine trip / MFIV and MSIV close	LPP + 0.0 sec
SIP on	PT-PZR-01 < 10.7MPa + 28sec delay
SIT on	PT-DC-01 < 4.03MPa
SIT low flow conversion	LT-SIT1,2,3,4-01 < 72.8, 72.6, 72.0, 72.2 %
SIT stop	LT-SIT1,2,3,4-01 < 47.4, 47.2, 46.6, 47.0 %
Secondary logic	
MSSV1,2-01 open	PT-SGSD1,2-01 > 8.1 MPa
MSSV1,2-01 close	PT-SGSD1,2-01 < 7.7 MPa
MSSV1,2-02 open	PT-SGSD1,2-01 > 8.3 MPa
MSSV1,2-02 close	PT-SGSD1,2-02 < 7.9 MPa
MSSV1,2-03 open	PT-SGSD1,2-01 > 8.48 MPa
MSSV1,2-03 close	PT-SGSD1,2-03 < 8.05 MPa
Aux. Feed Water open	LT-SGSDRS2-01 < 2.76m
Aux. Feed Water close	LT-SGSDRS2-01 > 3.61m
Aux. Feed Water Flow rate	0.2 kg/s

Table 5 Actual Initial and Boundary Condition for LTC-CL-04R Test

Design Parameter	Measured value/ STDEV*	Remark (Sensor ID)
Primary System		
Core Power (MW)	1.64/0.715	Heat loss: about 88 kW
Pressurizer Pressure (MPa)	15.5/0.0075	PT-PZR-01
Core Inlet Temperature (°C)	291.0/0.15	TF-LP-02G18
Core Outlet Temperature (°C)	326.8/0.11	TF-CO-07G14,18,21,25
Secondary System		
Steam Flow Rate per Each SG (kg/s)	0.382/0.031 0.425/0.001	SG-1 (QV-MS1-01) SG-2 (QV-MS2-01)
Feed Water Flow Rate per Each SG (kg/s)	0.410/0.001 0.413/0.003	SG-1 (QV-MF1-01, 2), SG-2 (QV-MF2-01, 2)
Feed Water Temperature (°C)	233.9/0.117 233.0/0.131	SG-1 (TF-MF1-01), SG-2 (TF-MF2-01)
Steam Pressure (MPa)	7.83/0.0005 7.83/0.0005	SG-1 (PT-SGSD1-01), SG-2 (PT-SGSD2-01)
Steam Temperature (°C)	295.6/0.101 295.6/0.075	SG-1 (TF-SGSD1-03), SG-2 (TF-SGSD2-03)
Secondary Side Level (m)	4.99/0.015 4.99/0.008	SG-1 (LT-SGSDRS1-01), SG-2 (LT-SGSDRS2-01)
Etc.		
Cold Leg Flow (kg/s)	1.98/0.062	Averaged Value for 4 CLs (QV-CL1A,1B,2A,2B-01B)
SIT temperature (°C)	12.2/0.188 12.7/0.143 14.2/0.147 14.0/0.250	SIT1 (TF-SIT1-03), SIT2 (TF-SIT2-03), SIT3 (TF-SIT3-03), SIT4 (TF-SIT4-03)

* STDEV: Standard deviation

Table 6 Actual Sequence of Events of LTC-CL-04R Test

Events	Timing (seconds)	Remarks
Break start	300	MFW terminated
MSSV	336/340	SG pressure
LPP trip	332	PT-PZR-01 < 12.48 MPa
SIP on	381	PT-PZR-01 < 10.7 MPa + 28sec delay
SIT on	1066	PT-DC-01 < 4.03 MPa
Loop seal clearing	733~3687 (1A) 754~3719 (2A)	
	4097~4151 (1A,1B) 4094~4160 (2B)	
	4982~5138 (1A) 4978~5150 (2A)	
	7322~ 7456 (1A)	

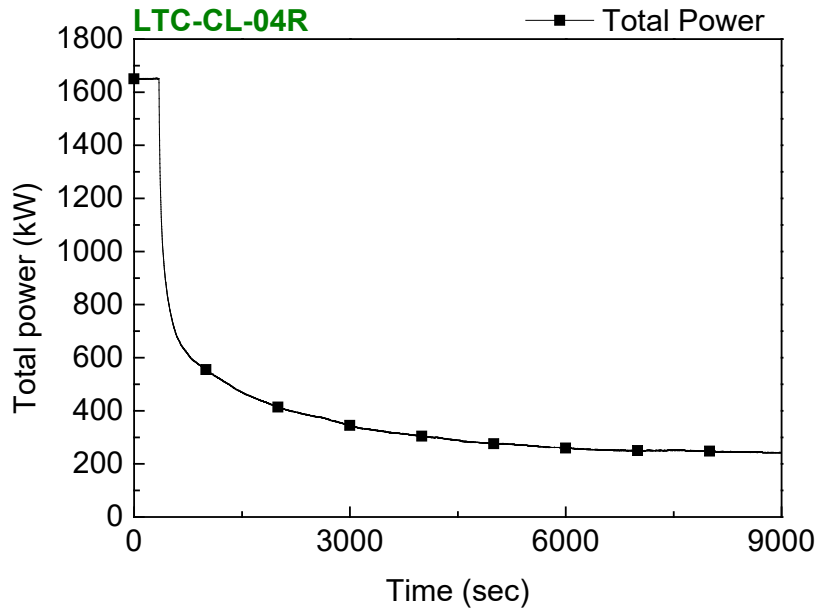


Figure 13 Decay Power for LTC-CL-04R Test

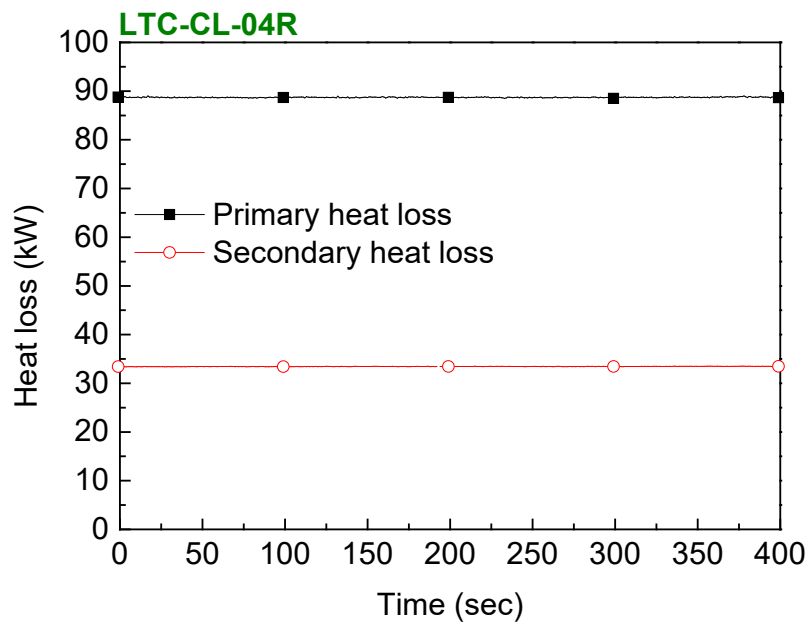


Figure 14 Estimated Heat Loss through System of LTC-CL-04R Test

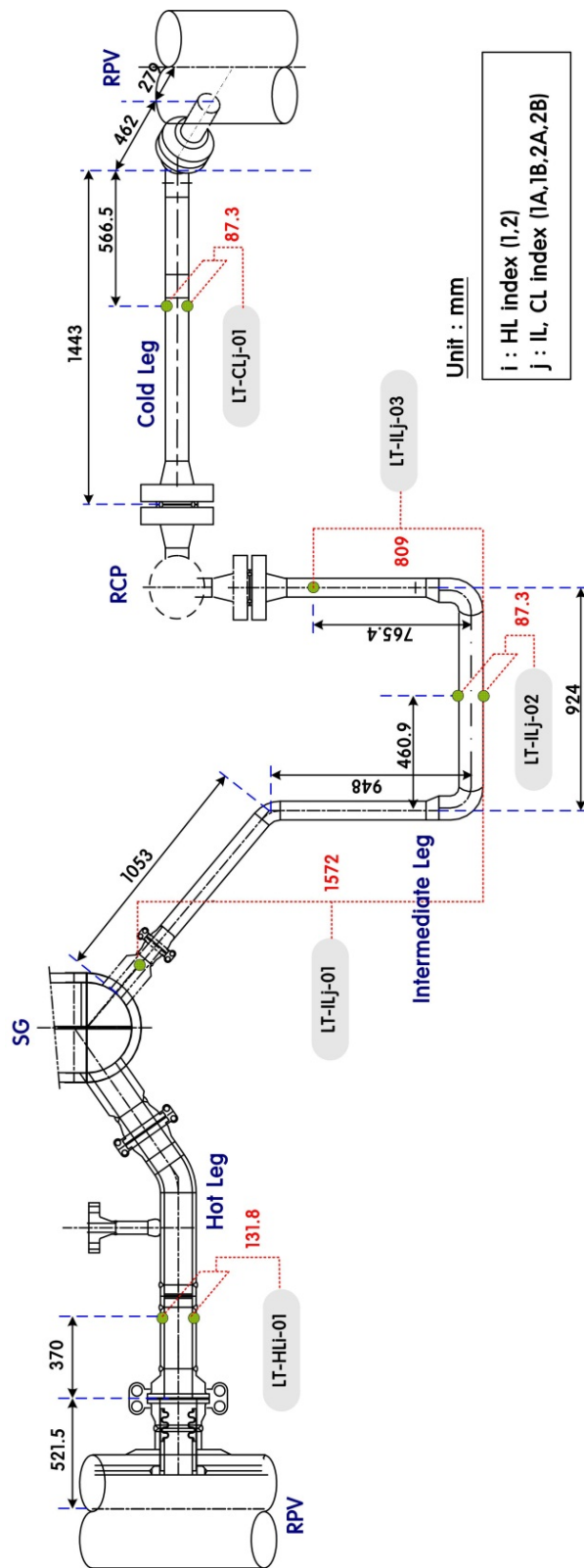


Figure 15 Diagram of Water Level Transmitter Installation at Intermediate Leg (j: Loop index, 1A, 1B, 2A, 2B)

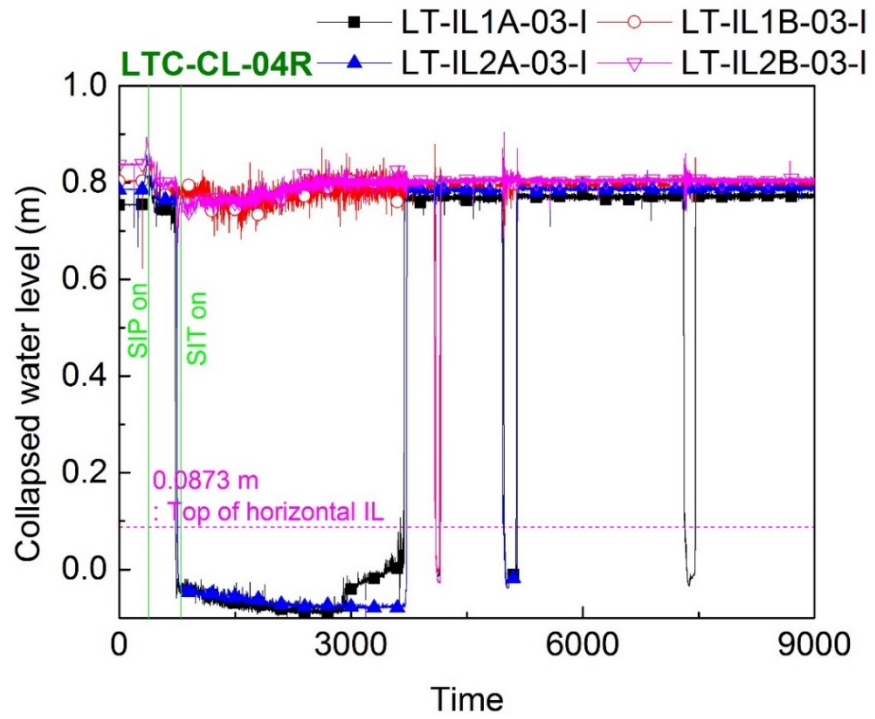


Figure 16 Water Level Behavior of LT-ILj-03 (j: Loop Index, 1A, 1B, 2A, 2B)

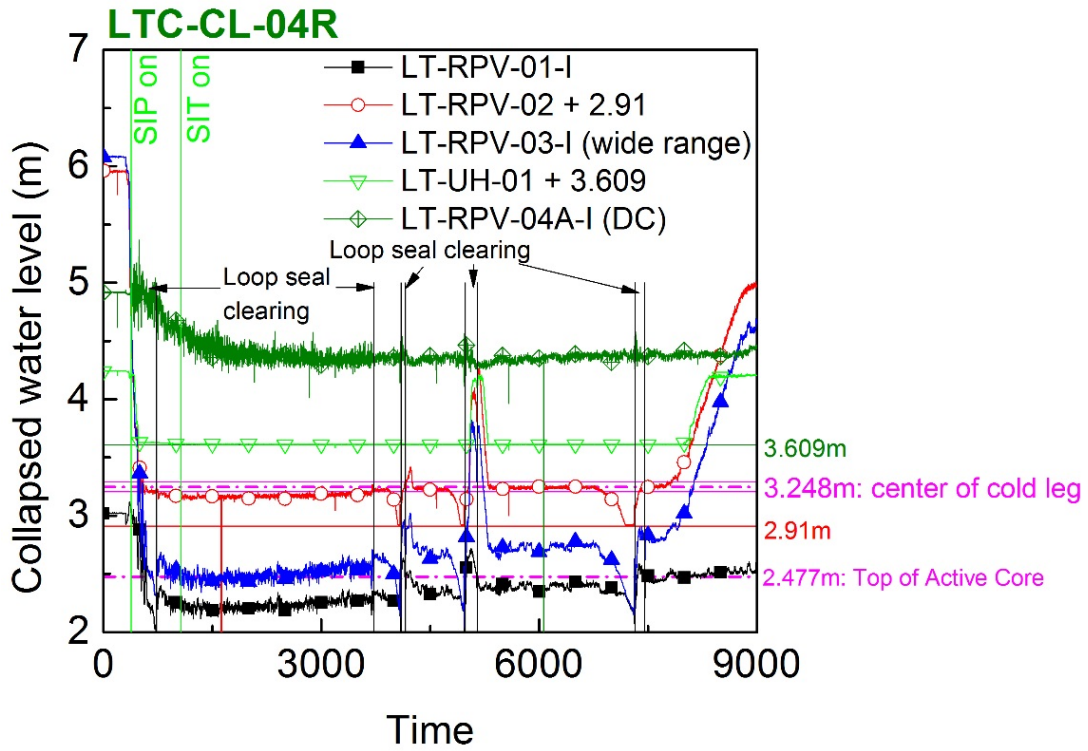


Figure 17 Water Level of Core and Downcomer of RPV

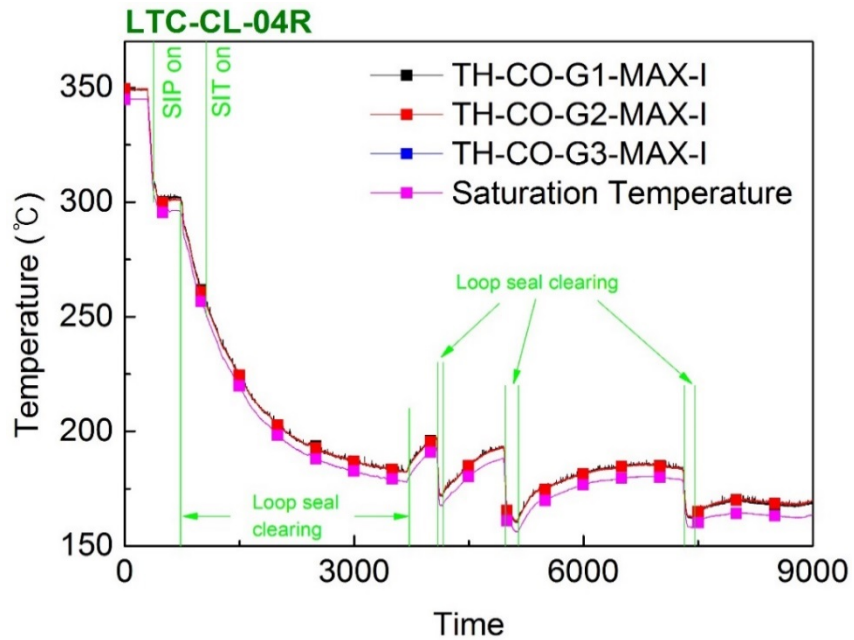


Figure 18 Core Temperatures and Saturated Temperature at Upper Head

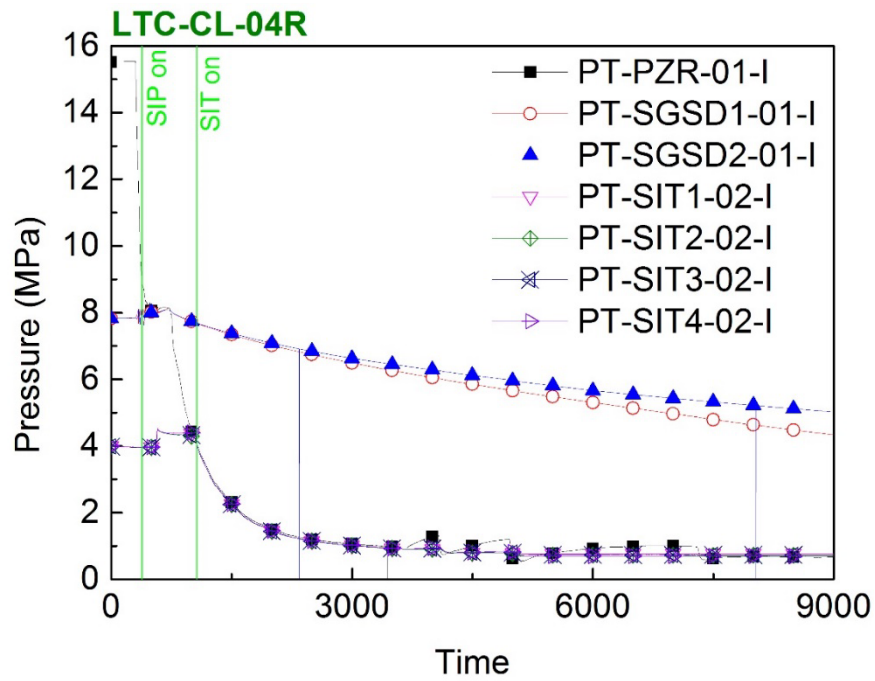


Figure 19 Pressure at Pressurizer, Steam Generators and SITs

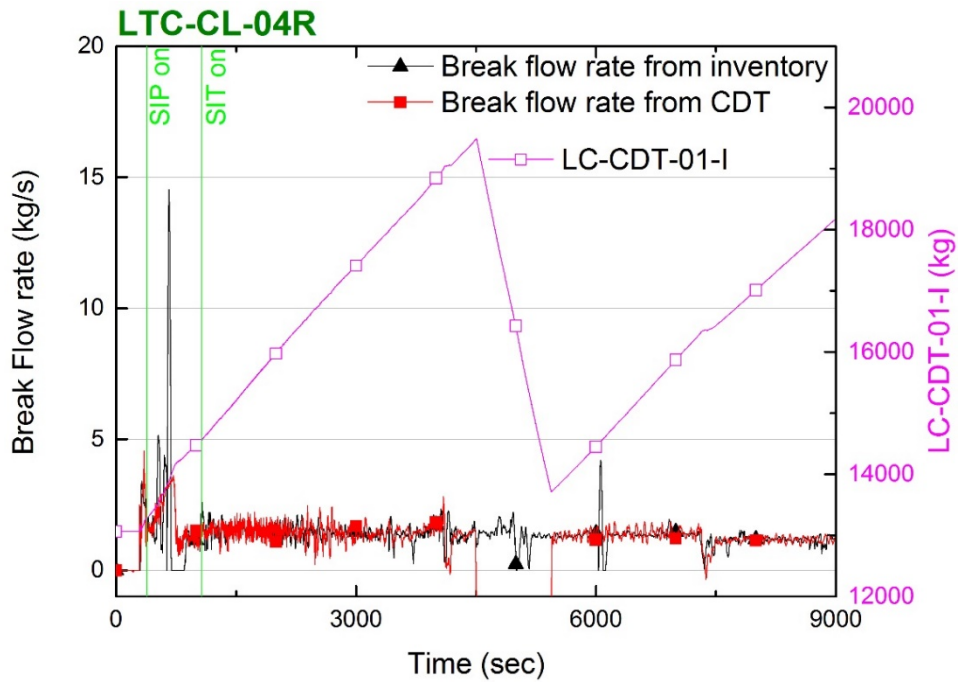


Figure 20 Condensation Tank Mass (LC-CDT-01-I) and Break Flow Rates (Triangle, Square)

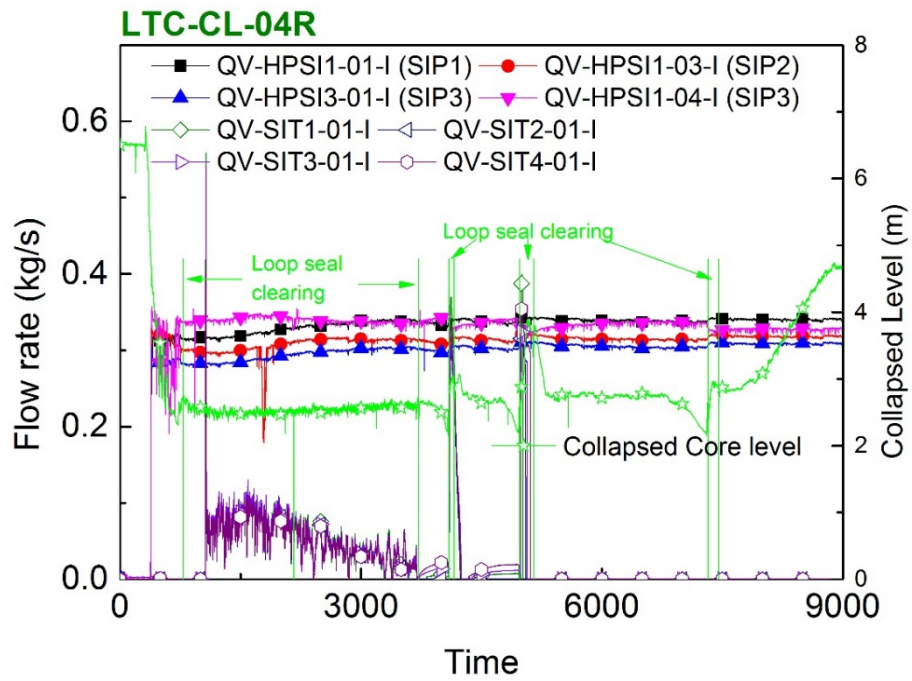


Figure 21 Flow Rate of SIPs and SITs

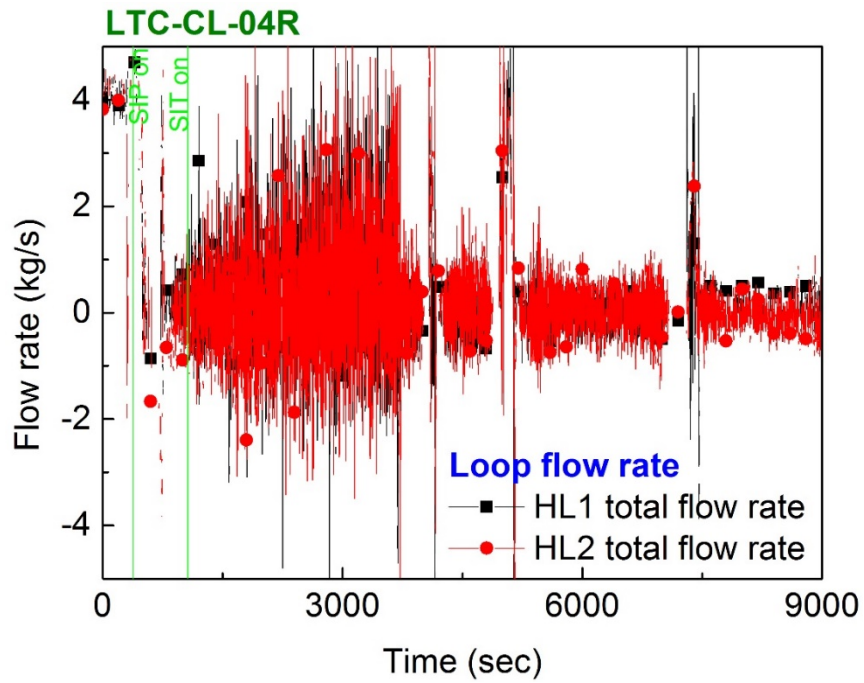


Figure 22 Flow Rate of Hot Legs

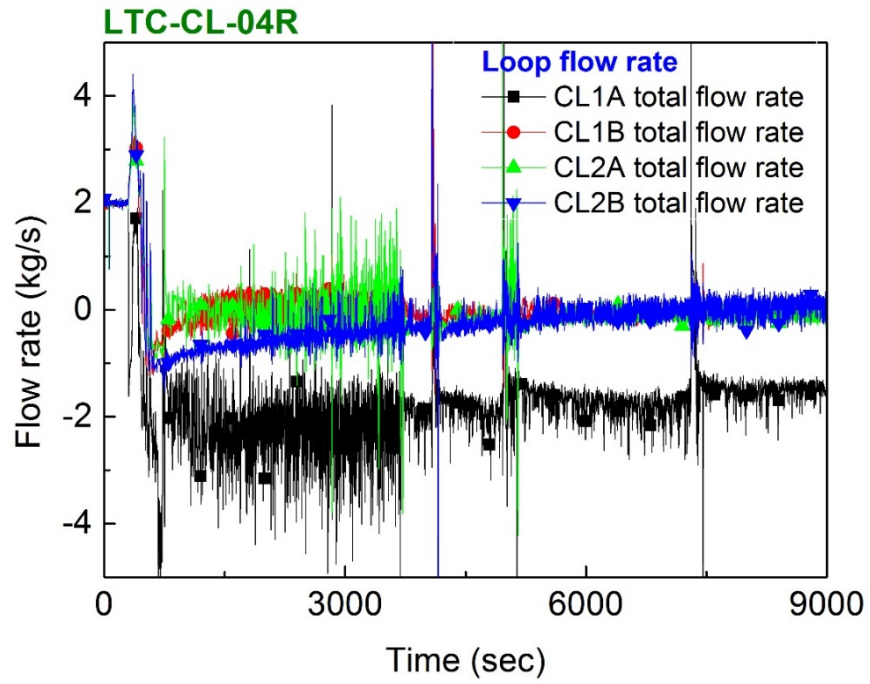


Figure 23 Flow Rate of Cold Legs

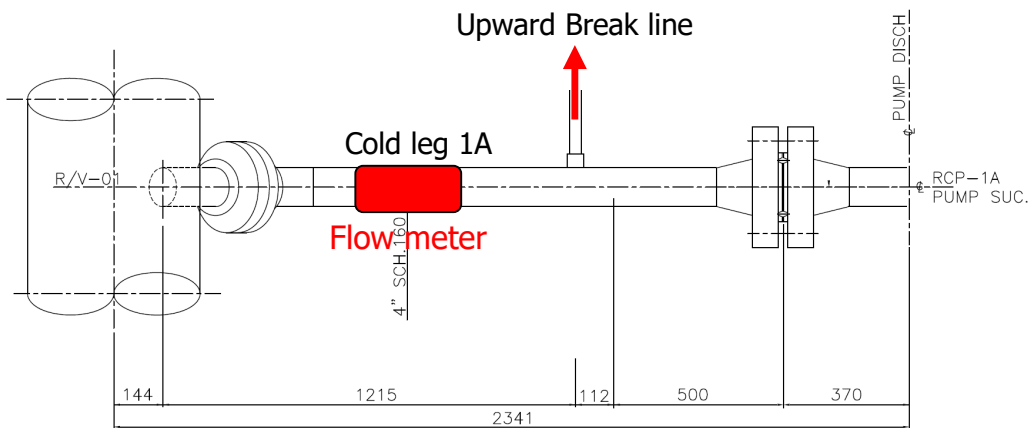


Figure 24 Location of Flow Meter of Cold Leg 1A

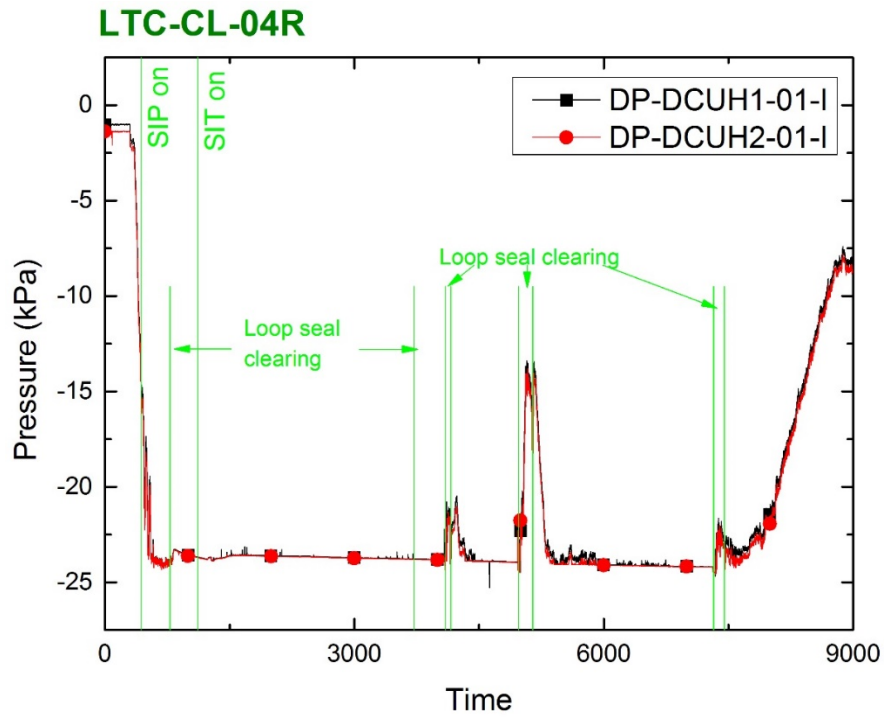


Figure 25 Differential Pressure between Downcomer and Upper Head

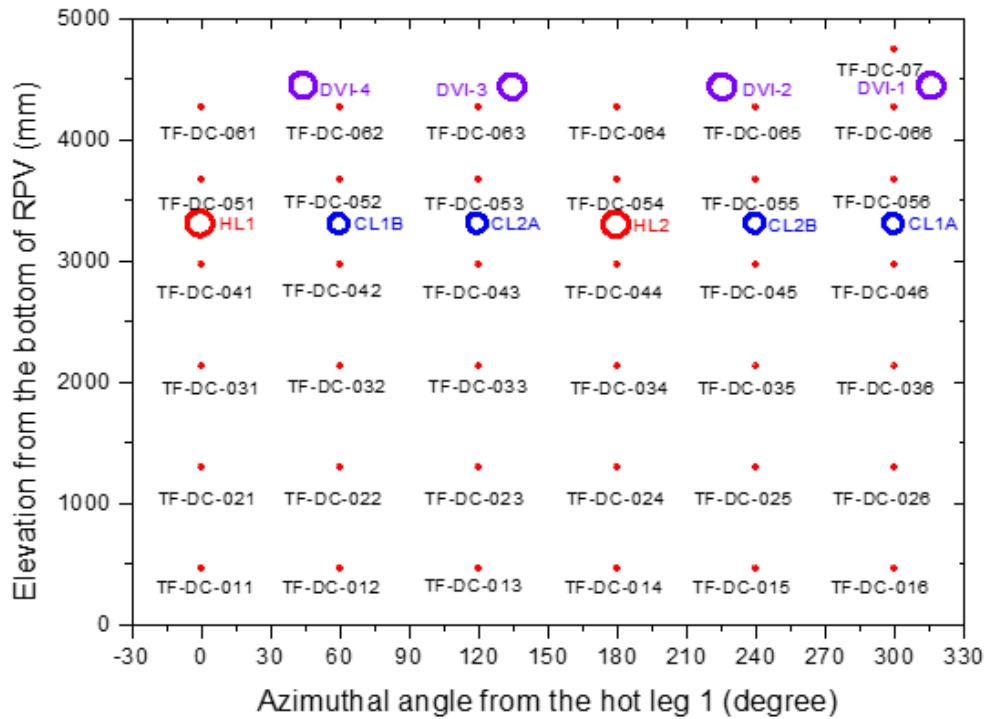


Figure 26 Thermocouple Distribution Map in Downcomer of RPV

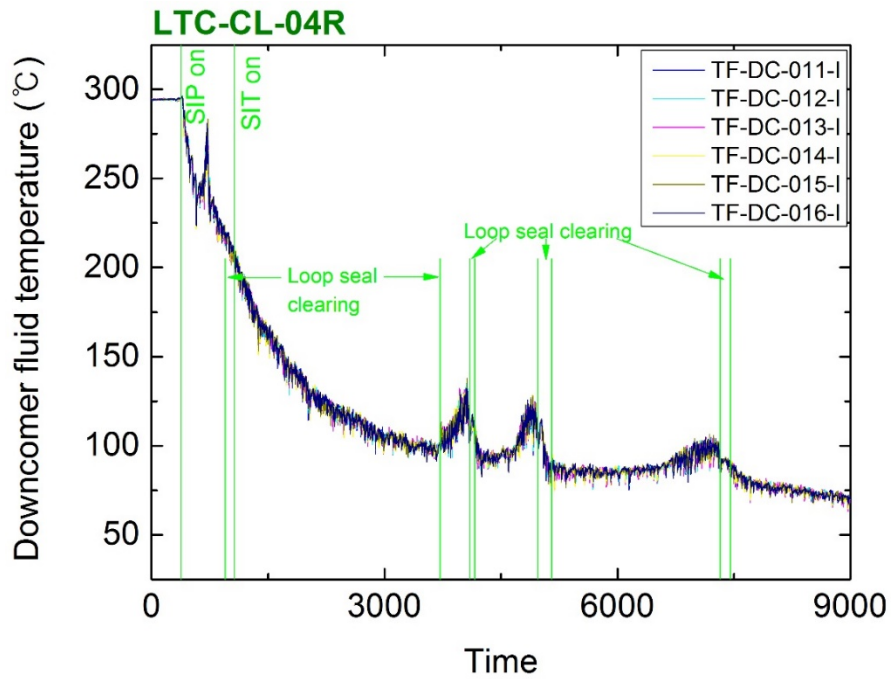


Figure 27 Temperature of Downcomer (TF-DC-011 ~ 016)

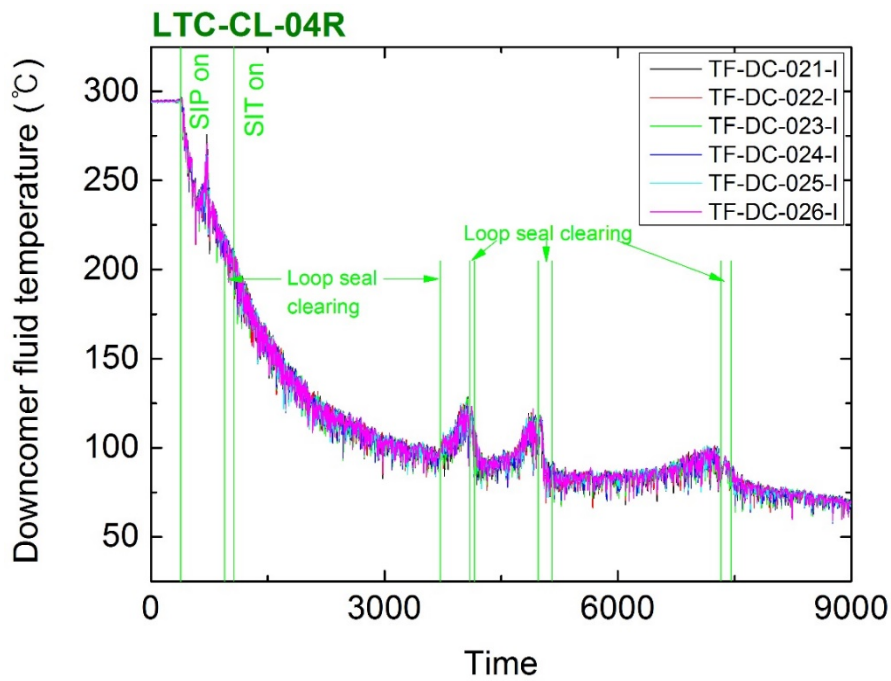


Figure 28 Temperature of Downcomer (TF-DC-021 ~ 026)

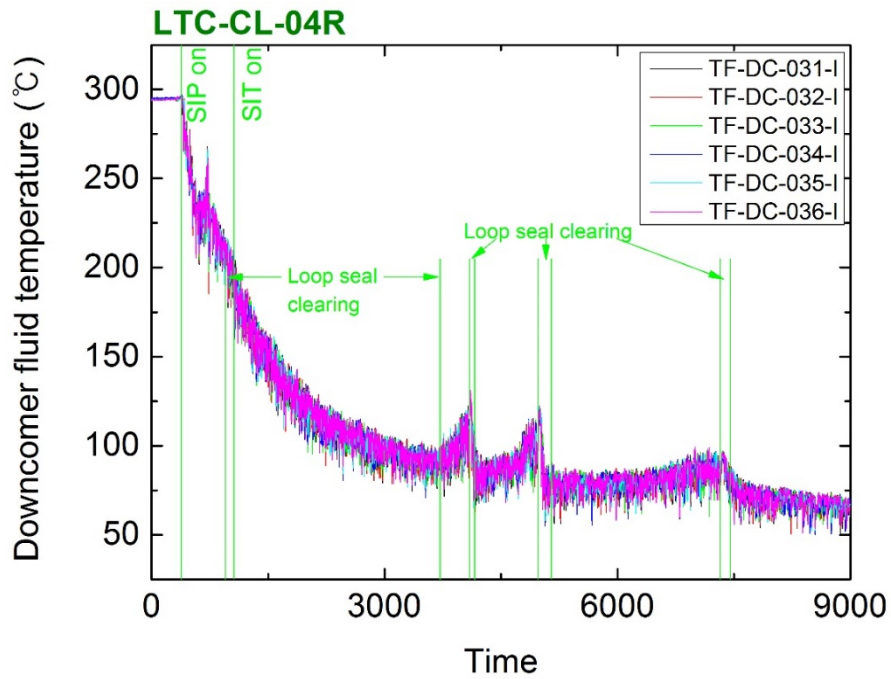


Figure 29 Temperature of Downcomer (TF-DC-031 ~ 036)

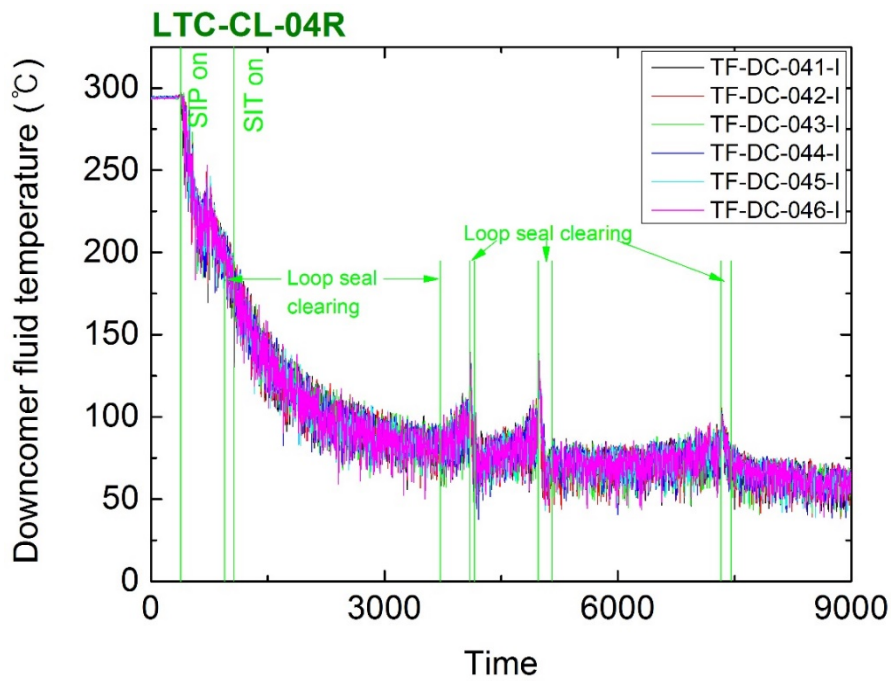


Figure 30 Temperature of Downcomer (TF-DC-041 ~ 046)

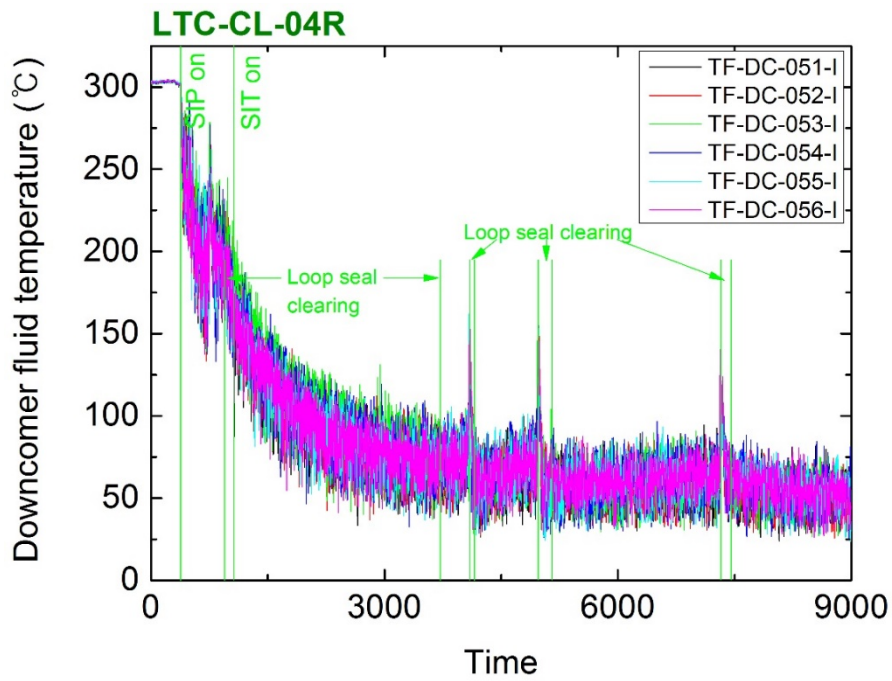


Figure 31 Temperature of Downcomer (TF-DC-051 ~ 056)

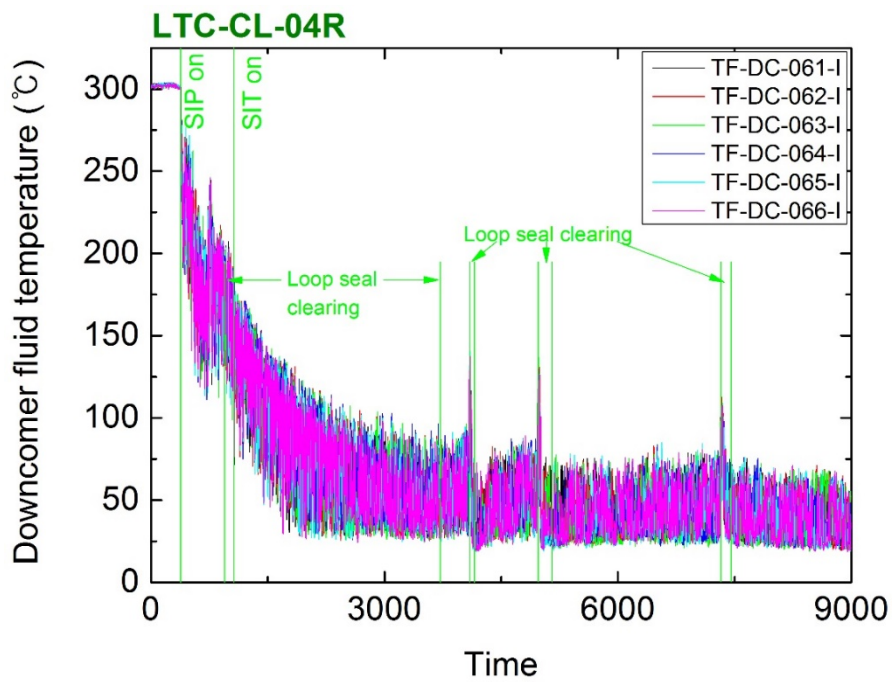


Figure 32 Temperature of Downcomer (TF-DC-061 ~ 066)

3 RELAP5 INPUT MODELS

3.1 RELAP5 Input Model for ATLAS Simulation

3.1.1 RELAP5 Nodalization for ATLAS Facility

KAERI has developed a standard input model for the ATLAS facility. The latest ATLAS input model for a steady state condition is shown in Figure 33. In order to simulate a break in a cold leg, a break line was added on the top of component 381 (C381) located between the RPV and the RCP of CL-1A. In addition, an upward facing break was modelled using off-take model applied to an affected junction from C381. Except for a break line, any node subdivision was not applied in this study. As passive safety components, safety injection tanks were modelled as accumulators equipped with fluidic device. SITs were connected to the direct vessel injection line of RPV annular shroud.

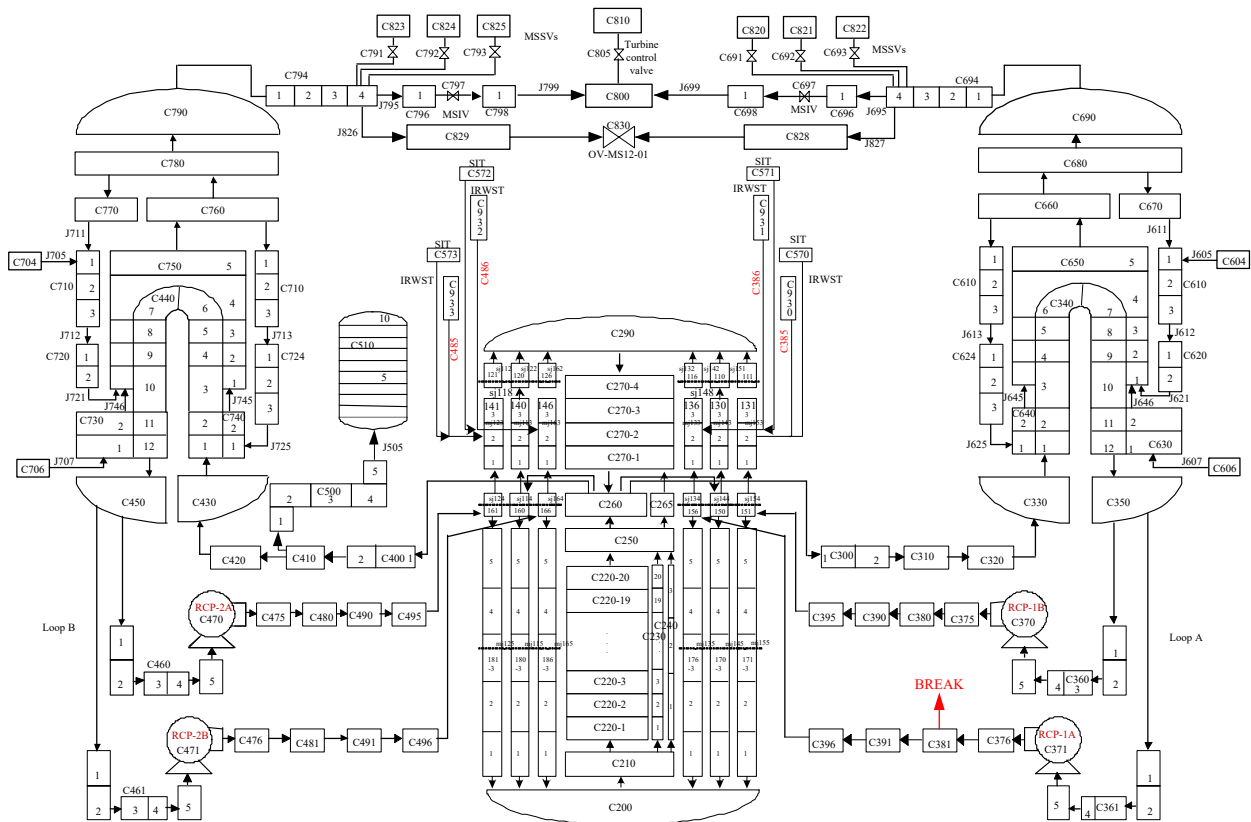


Figure 33 ATLAS Nodalization of SBLOCA (or IBLOCA)

3.1.2 Break Modeling

It should be noted that a shape of slot break having a very slim line with narrow width is hardly made in the test and modelled in one-dimensional (1-D) codes including the RELAP5 code. Thus, the break shape in the test and the present code calculation was simulated as a single hole using a nozzle that has an inner diameter of 7.12 mm and a length of 100 mm.

In order to predict accurate behavior of break flow against the test data, a break line needs to be modelled same with the test configuration as mentioned in section 2.1.2 . Figure 34 shows nodalization of a break line. The 1-D break line consists of a break main line, a break nozzle, break valve (trip valve), and sink volume. Among those components, modeling of the break nozzle is the most important in this simulation since choking in a single break line occurs at the smallest area of the break line. Compared to the break main line having an inner diameter of 33.99 mm, the break nozzle and the break valve have the smallest inner diameter of 7.12 mm. Thus, choking is expected to occur at the valve which is diverging the area of the break nozzle. Choking condition was only applied to this part.

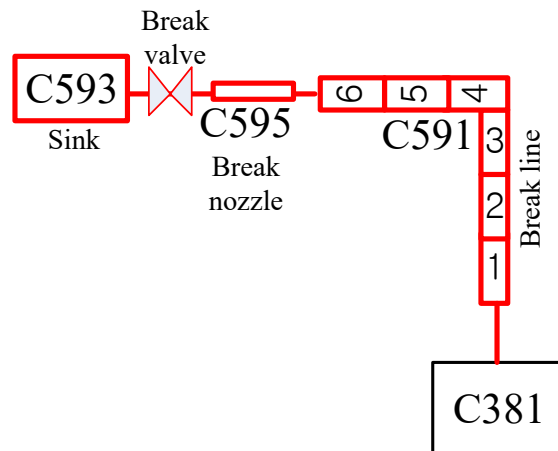


Figure 34 Nodalization of Break Line

4 RESULTS

4.1 ATLAS Calculations and Discussions

The RELAP5 calculation data were compared against the test data and the results are shown in Figure 35 through Figure 46. The ATLAS test data are labeled as “Exp” and the RELAP5 calculation data are labeled as “RELAP5”.

RELAP5 calculation shows a reasonable agreement with the test result for the primary loop pressure, as presented in Figure 35. The predicted times of the first and the second pressure drop are similar with the test data during an early stage of the test. After the second pressure drop, RELAP5 calculated relatively higher pressure because the break flow rates of RELAP5 calculation were less than those of the test during this period. In Figure 37, the break flow rates are compared. RELAP5 predicted larger break flow rates than those of the test before 800 seconds and the calculated accumulated mass of break flow was also larger than that of the test during an early period before 800 seconds. After 800 seconds, calculated break flow rates were larger than those of the test and it induced a less accumulated break flow and a higher primary pressure.

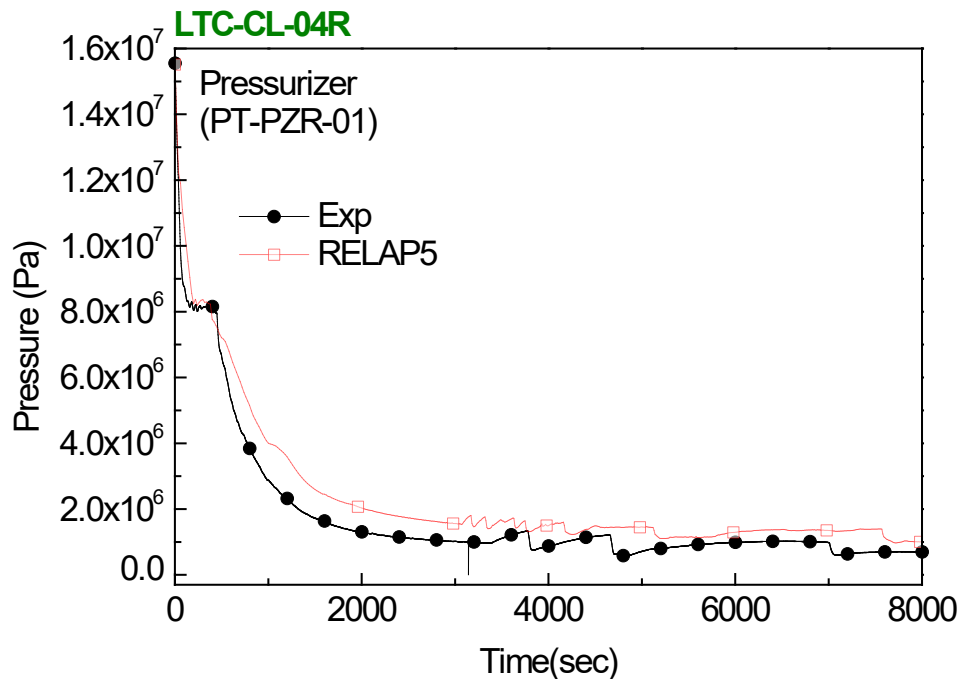


Figure 35 Pressurizer Pressure

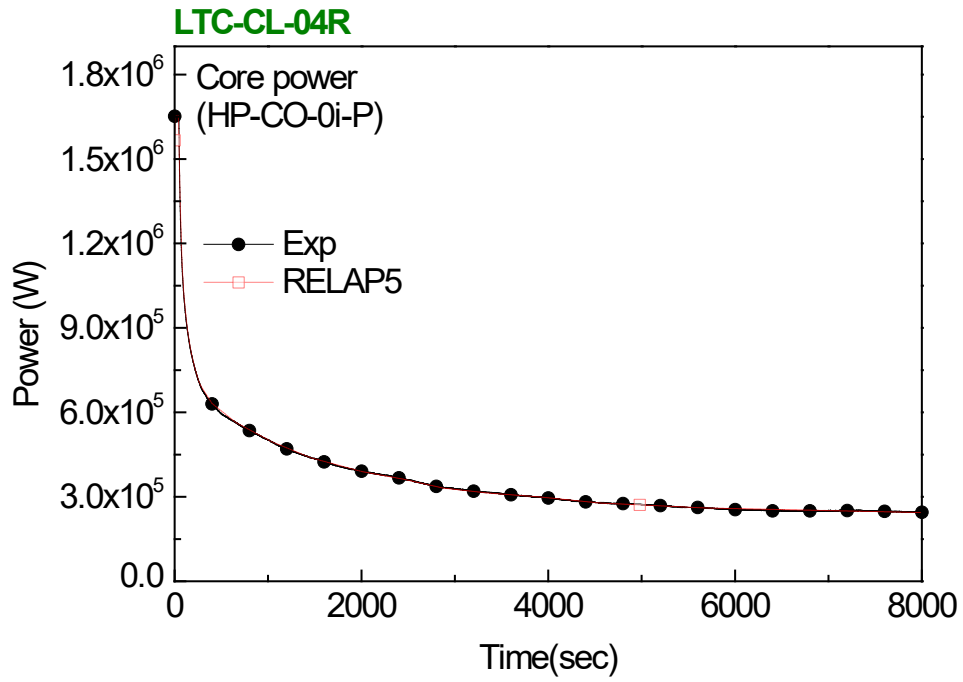


Figure 36 Core Power

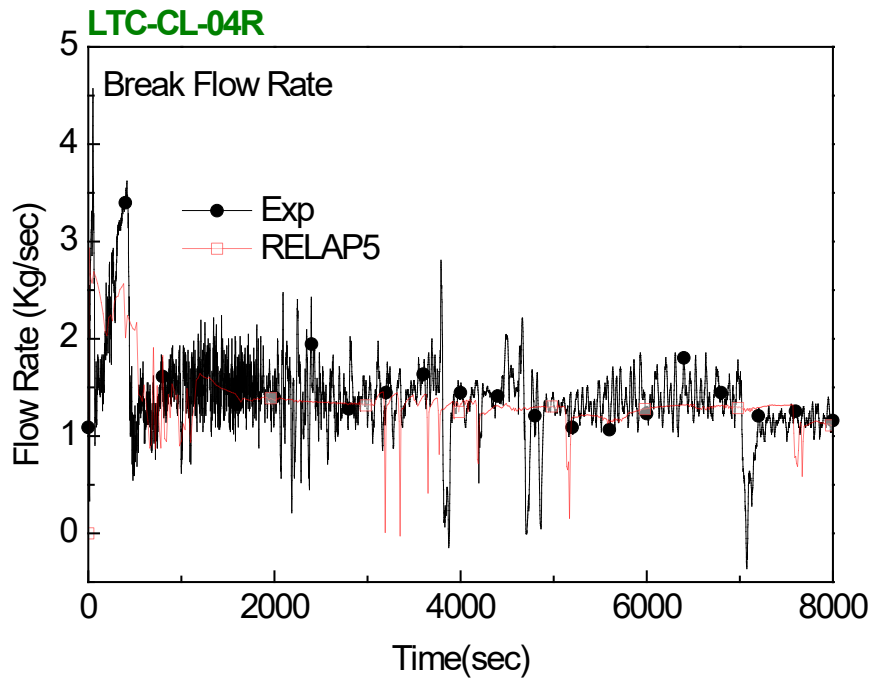


Figure 37 Break Flow Rate

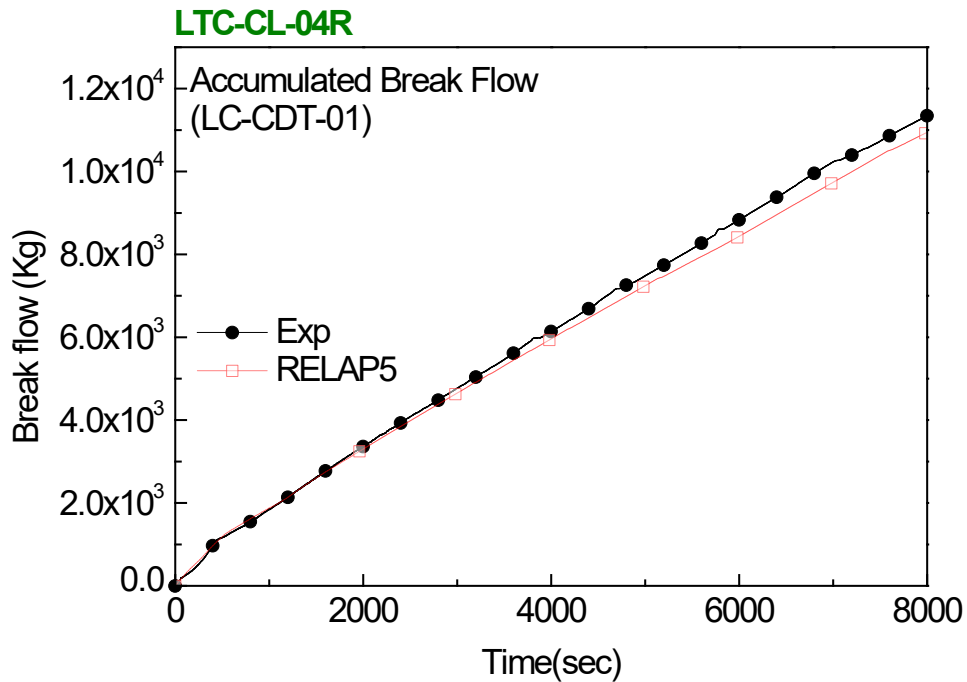


Figure 38 Accumulated Break Flow

RELAP5 analysis reasonably predicted the core collapsed water level as shown in Figure 39. The core collapsed water level sharply increased at the loop seal clearing because the water in the loop seal flowed into the core. On the other hands, the core collapsed water level gradually decreased after the loop seal reformation due to the evaporation at the core. The loop seal clearing and reformation times of RELAP5 calculation were different from those of the test. And this discrepancy made a different oscillation pattern of the core collapsed water level. However, the overall trend of collapsed water level was similar in both the test and the RELAP5 calculation.

The maximum heater wall temperatures are presented in Figure 40. In both data, temperature reaches its peak after every loop seal reformation. The reason for the peak of temperature is attributed to the increase of saturated temperature at the core. After loop seal reformation, the evaporated steam at the core was accumulated at the upper head and so the upper head pressure increased gradually. The increased pressure led to the increase of the saturated temperature of the coolant at the core. Therefore, the heater wall temperatures also increased with the increase of the saturated temperature of the coolant at the core. It could be found from the RELAP5 calculation that a loop seal reformation does not induce an excursion of the cladding temperature which is also observed in the ATLAS test.

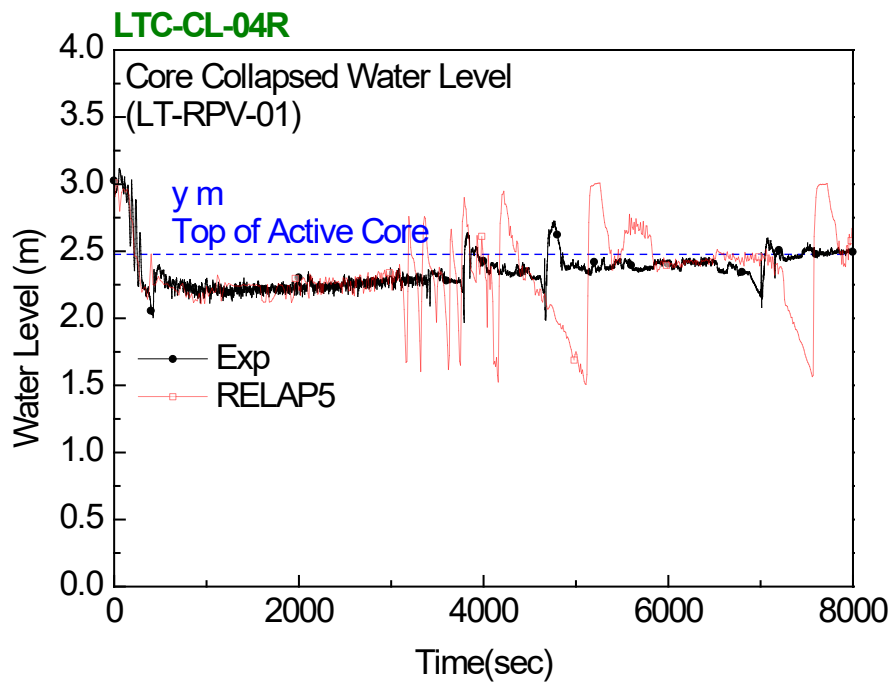


Figure 39 Core Collapsed Water Level

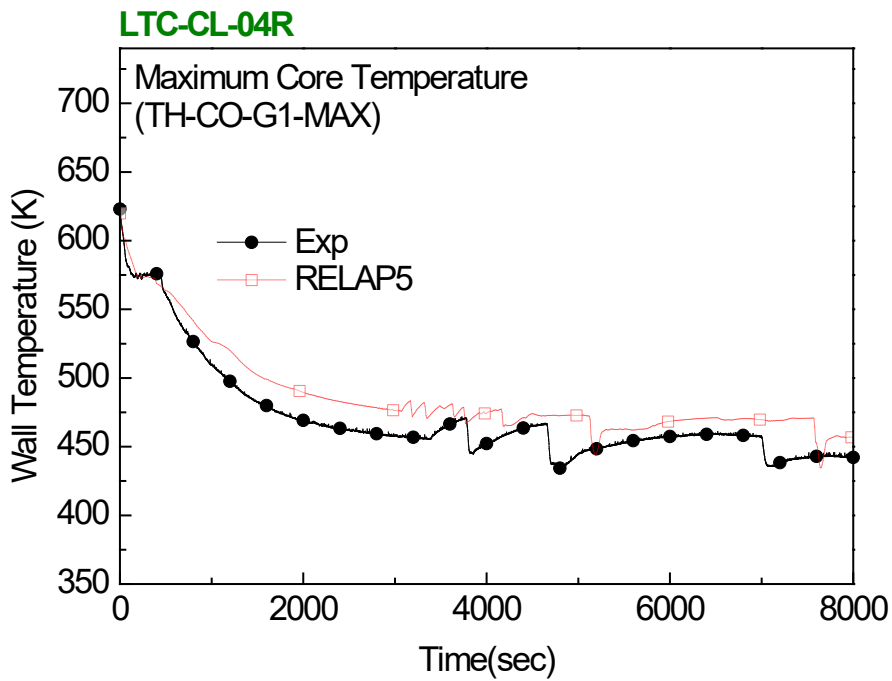


Figure 40 Maximum Core Temperature

The secondary system pressures of both steam generators are presented in Figure 41 and Figure 42, respectively. RELAP5 calculation over-predicted the secondary system pressure due to non-application of a heat loss model to the secondary side of the steam generator. This led to under-prediction of the cooling rate and the depressurization rate at steam generators.

The discrepancy of the secondary system pressures between the two steam generators was relatively larger in the RELAP5 calculation compared to the ATLAS test. The reason for this discrepancy can be attributed to the different flow rates between the loops. Figure 43 and Figure 44 show the flow rates at the hot legs. In the test, the flow rates were similar for both loops. However, the flow rate at hot leg 1 was almost zero in the RELAP5 calculation. The Coolant flow rate at the loop is the most important parameter for evaluating the heat transfer characteristics. The relatively small flow rate at hot leg 1 indicates that the heat transfer rate at the steam generator 1 was smaller than that at the steam generator 2.

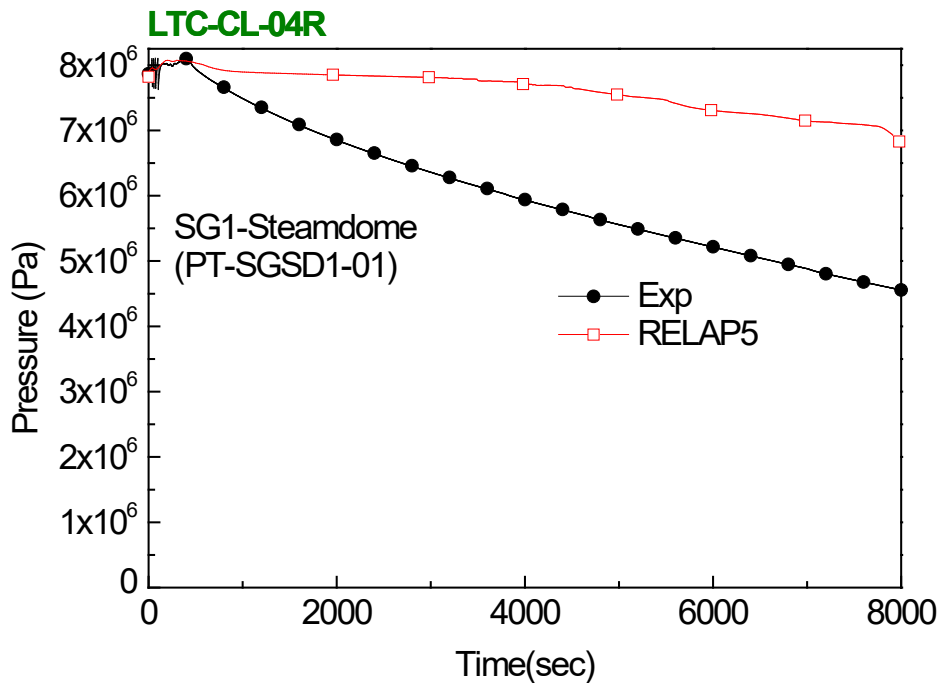


Figure 41 Steam Dome Pressure of Steam Generator-1

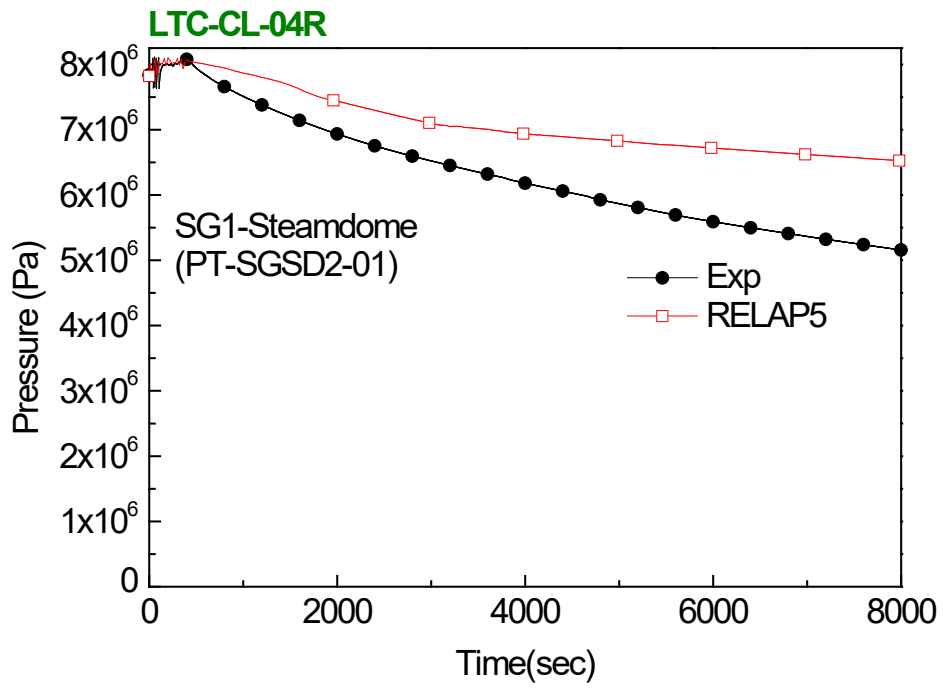


Figure 42 Steam Dome Pressure of Steam Generator-2

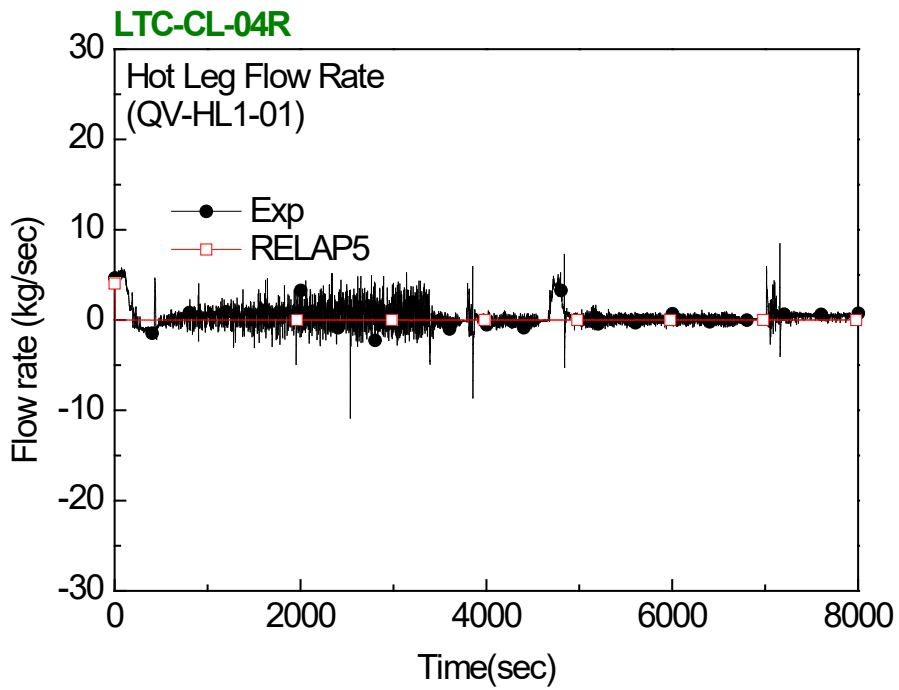


Figure 43 Hot Leg-1 Flow Rate

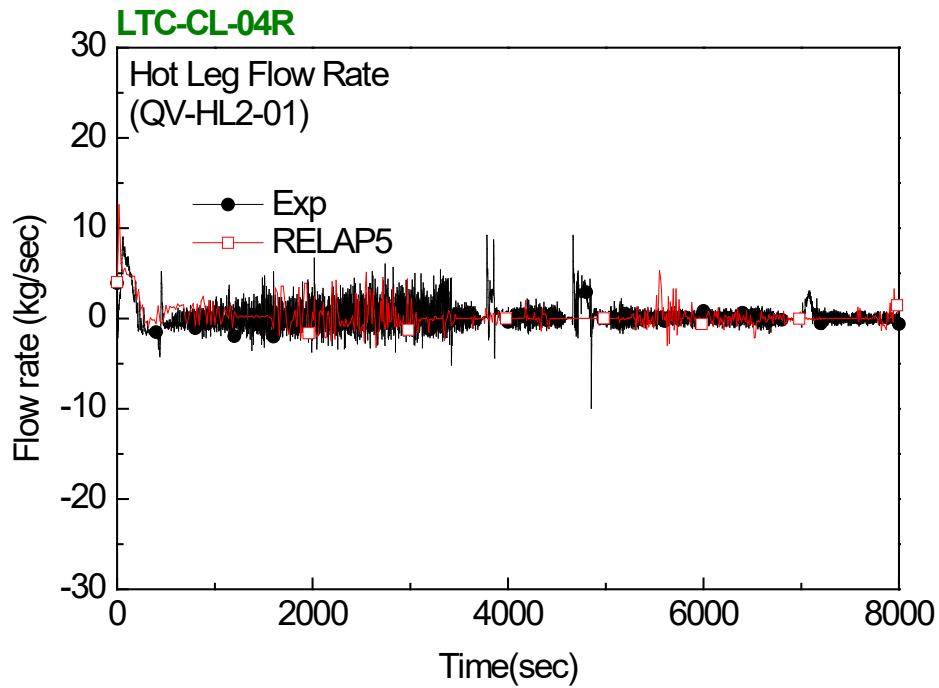


Figure 44 Hot Leg-2 Flow Rate

To compare the characteristics of loop seal clearing and reformation, the collapsed water levels of intermediate legs are presented in Figure 45 and Figure 46. If the water level of the vertical intermediate leg is lower than the horizontal dash line, which marks the height of the horizontal pipe at the intermediate leg, this loop seal can be assumed to be cleared. RELAP5 calculation cannot predict the exact time for loop seal clearing and reformation. However, the calculation predicted similar trends for loop seal clearing and reformation. Duration of loop seal clearing for the early stage was longer than that of the long-term stage and loop seal cleared more times for the early phase than those of the long-term phase.

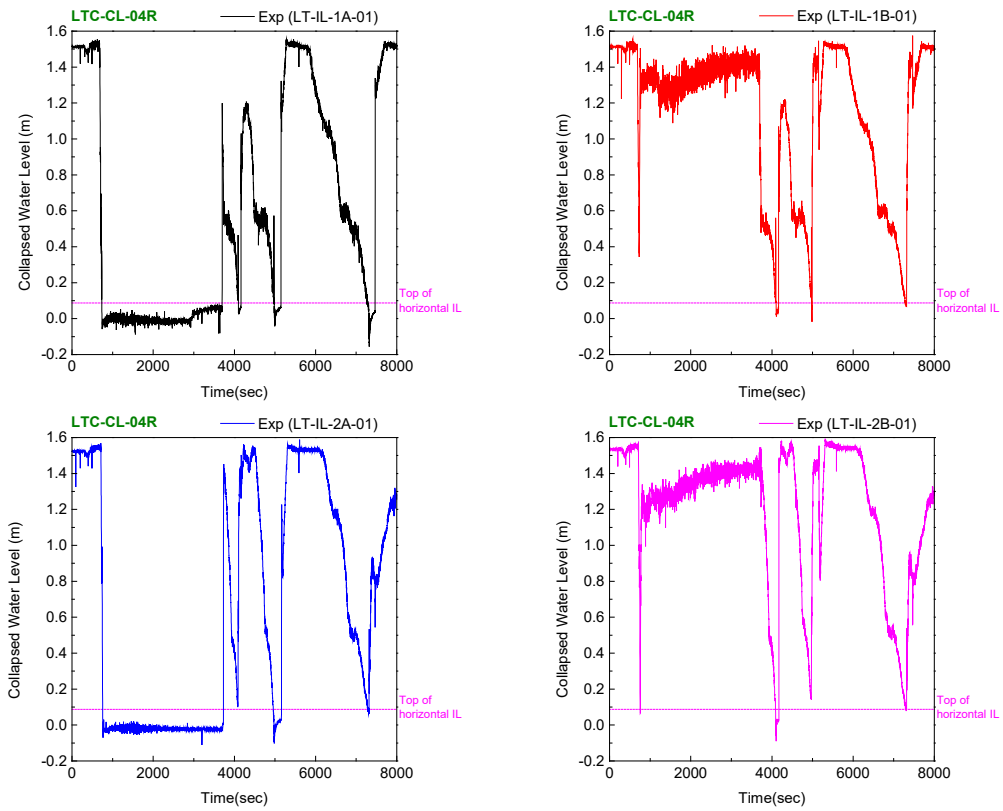


Figure 45 Collapsed Water Level at Vertical Intermediate Leg (Exp.)

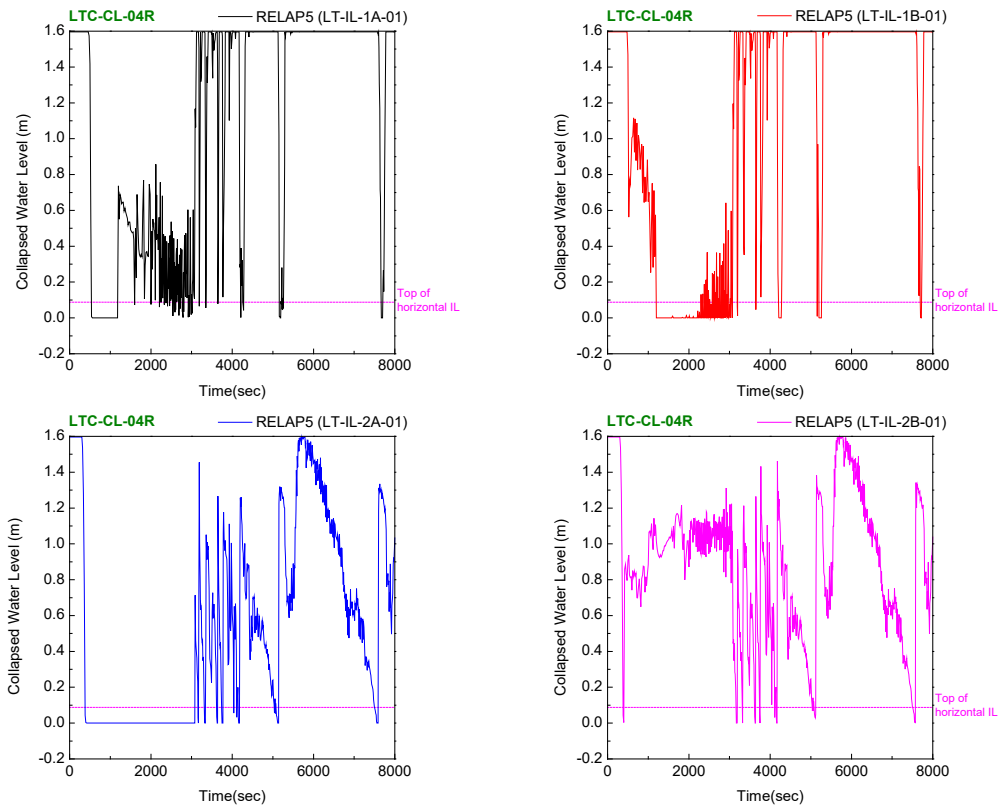


Figure 46 Collapsed Water Level at Vertical Intermediate Leg (RELAP5)

5 RUN STATISTICS

The calculations were performed using Intel® Core™ i7-6700 @ 3.40 GHz processor. The operating system is Windows 7 Enterprise K. Table 7 shows the run statistics for the RELAP5 calculation.

Table 7 Run Statistics

Code	Transient Time (s)	CPU Time (s)	CPU/Transient Time	Number of Time Steps
RELAP5 Mod3.3 Patch5	8000.0	41945.3	5.24	41945.3

6 CONCLUSIONS

The ATLAS test for 4-Inch cold leg top-slot break LOCA was calculated using the RELAP5 Mod3.3 Patch5 code. Focused on the loop seal clearing and reformation phenomena, the calculation results were compared to the test data. In general, the RELAP5 calculation results show a reasonable agreement with the ATLAS test data. The RELAP5 code predicted repeatable loop seal clearing and reformation which was observed in the ATLAS test. The loop seal clearing and reformation led no excursion of the cladding temperature during the transient in both the test and the RELAP5 calculation. There are discrepancies in prediction of the secondary system pressure at steam generators. The reason for these discrepancies could be attributed to non-application of a heat loss model to the steam generator. In terms of the overall trend for loop seal behavior, the calculation shows a good agreement with the ATLAS data, but a detailed timing of loop seal clearing and reformation shows a discrepancy between the test and the calculation.

7 REFERENCES

- [1] Kim, J. Kang, K.-H., Choi, K.-Y., Park, Y.-S., Bae, B.-U., Choi, N.-H., Min, K.-H., Shin, Y.-C., 2016. Analysis Report on the Long Term Cooling Test for Cold leg Top Slot Break, Korea Atomic Energy Research Institute Technical Report, KAERI/TR-6605/2016
- [2] Baek W.-P. Song, C.-H., Yun, B.-J., Kwon, T.-S., 2005. KAERI Integral Effect Test Program and ATLAS Design, Nuclear Technology 152, pp.183-195.
- [3] Ishii, M., Kataoka I., 1983. Similarity Analysis and Scaling Criteria for LWRs Under Single Phase and Two-Phase Natural Circulation, NUREG/CR-3267, ANL-83-32, Argonne National Laboratory.
- [4] Choi, K.-Y. Kang K.-H., Kwon, T.-S., Kim Y.-S., Kim, J., Moon, S.-K., Park, Y.-S., Park H.-S., Bae, B.-U., Song, C.-H., Yi, S.-J., Cho, S., Yun, B.-J., 2014. Scaling Analysis Report of the ATLAS Facility, Korea Atomic Energy Research Institute Technical Report, KAERI/TR-5465/2014.
- [5] Lee, J.B., Bae, B.-U., Park, Y.-S., Kim, J., Kim Y.-S., Cho, S., Jeon, W., Park H.-S., Yi, S.-J., Moon, S.-K., Choi, K.-Y., Song C.-H. Choi, N.-H., Shin, Y.-C., Min, K.-H., Kang K.-H., 2018, Description report of ATLAS facility and instrumentation (second revision), Korea Atomic Energy Research Institute Technical Report, KAERI/TR-7218/2018.

BIBLIOGRAPHIC DATA SHEET

(See instructions on the reverse)

NUREG/IA-0523

2. TITLE AND SUBTITLE

**Evaluation for 4-Inch Cold Leg Top-Slot Break LOCA in ATLAS Facility
with RELAP5 Mod3.3 Patch5**

3. DATE REPORT PUBLISHED

MONTH

January

YEAR

2021

4. FIN OR GRANT NUMBER

5. AUTHOR(S)

J. Kim, K.-H. Kang, B.-U. Bae, Y. Park*, A. Shin, M. Cho**

6. TYPE OF REPORT

Technical

7. PERIOD COVERED (Inclusive Dates)

8. PERFORMING ORGANIZATION - NAME AND ADDRESS (If NRC, provide Division, Office or Region, U. S. Nuclear Regulatory Commission, and mailing address; if contractor, provide name and mailing address.)

Korea Atomic Energy Research Institute, 111, Daedeok-daero 989beon-gil, Yuseong-gu, Daejeon, Korea*
Korea Institute of Nuclear Safety, 62, Gwahak-ro, Yuseong-gu, Daejeon 34142, Republic of Korea**

9. SPONSORING ORGANIZATION - NAME AND ADDRESS (If NRC, type "Same as above", if contractor, provide NRC Division, Office or Region, U. S. Nuclear Regulatory Commission, and mailing address.)

Division of Systems Analysis
Office of Nuclear Regulatory Research
U.S. Nuclear Regulatory Commission
Washington, D.C. 20555-0001

10. SUPPLEMENTARY NOTES

K. Tien, NRC Project Manager

11. ABSTRACT (200 words or less)

The present works, an ATLAS test for 4-Inch cold leg top-slot break LOCA and a simulation of this test with RELAP5 Mod3.3 Patch4, are presented and the calculation results are compared and discussed against the test data. An ATLAS model for RELAP5 was applied for steady state. And then, a transient calculation was performed with a break line model that was developed for the present work. The RELAP5 calculations show a reasonable agreement with the test data. Especially, the RELAP5 predicted repeatable loop seal clearing and reformation in the test. The loop seal clearing and reformation led no excursion in the cladding temperature in both the test and RELAP5 calculation.

12. KEY WORDS/DESCRIPTORS (List words or phrases that will assist researchers in locating the report.)

RELAP5, ATLAS, Cold-leg break LOCA

13. AVAILABILITY STATEMENT

unlimited

14. SECURITY CLASSIFICATION

(This Page)

unclassified

(This Report)

unclassified

15. NUMBER OF PAGES

16. PRICE



Federal Recycling Program



**UNITED STATES
NUCLEAR REGULATORY COMMISSION
WASHINGTON, DC 20555-0001**

OFFICIAL BUSINESS



@NRCgov

NUREG/IA-0523

**Evaluation for 4-Inch Cold Leg Top-Slot Break LOCA in ATLAS
Facility with RELAP5 Mod3.3 Patch5**

January 2021